

KARMA



Karst Aquifer Resources availability and quality in the **Mediterranean Area**

Recharge evaluation

Deliverable 2.2

Authors (by alphabetical order):

Bartolomé Andreo Navarro (UMA), Juan Antonio Barberá Fornell (UMA), Zhao Chen (KIT), Guillaume Cinkus (UMO), Joanna Doummar (AUB), Nikolai Fahrmeier (KIT), Jaime Fernández Ortega (UMA), Nico Goldscheider (KIT), Hervé Jourde (UMO), Valeria Lorenzi (URO), Ana Isabel Marín Guerrero (UMA), José Francisco Martín Rodríguez (UMA), Jihad Othman (AUB), Marco Petitta (URO) and Chiara Sbarbati (URO)

Date: May 2021



This project has received funding from the European Union's PRIMA research and innovation programme



Project Partners



(Coordinator)



SAPIENZA
UNIVERSITÀ DI ROMA



Executive Summary

WP2 deals with the evaluation of water availability at the five test sites in KARMA project using different methods. The previous deliverable (D2.1 Preliminary water budget) consisted of a preliminary assessment of the water balance (recharge/discharge) in individual test sites, using available data and (recent and historical) information. Thus, a first estimation of karst groundwater resources was established.

The present deliverable (D2.2 Recharge evaluation) comprises the core activity of the Task 2.1 “Recharge assessment and tracer tests”, and it includes an updated estimation of recharge rates in the KARMA test sites. The final goal is to provide a distributed recharge map for the studied areas at a catchment scale in a continental Mediterranean context. Therefore, a more accurate recharge assessment was performed in each study area, as described in the following chapters.

The common research approach consisted of the application of the APLIS method, originally developed by members of the UMA partner (Andreo et al., 2008; Marin, 2009). This method was developed from the study of eight representative carbonate aquifers in Andalusia (S Spain), using information available on databases maintained by government bodies. The application of APLIS at different test sites different from the climatic and hydrogeological contexts in which the method was originally designed also serves as a test of its robustness and reliability.

In a further step, provided results on the spatial distribution of aquifer recharge will be compared with discharge measurements for the investigated karst systems. Besides APLIS, alternative approaches (i.e. hydraulic modeling) have been performed in some individual test sites for the same purpose.

In the following sections, the main results of recharge assessment in almost all study areas are shown and, in the final stage, potential method improvements are criticized to allow the correct implementation of the following WP2-related activities, also contributing to WP3 and WP4. Despite slight differences regarding total recharge volume in KARMA aquifers, the APLIS method has proved to be a consistent tool for recharge estimation.

The main limitations derived from APLIS application in KARMA test sites are related to (1) the effect in the net recharge of the permanent snow cap, resulting in a reduction of the infiltration rate; (2) impermeable areas, such as those affected by anthropic modifications that practically make the infiltration negligible, and (3) remarkable discrepancies in calculations during dry periods, in which evapotranspiration through vegetation seem to be higher.

Table of contents

Technical References	1
Version History	1
Project Partners	1
Executive Summary.....	1
1 Introduction.....	4
2 The APLIS method: general aspects	5
3 Gran Sasso aquifer (Case Study Italy).....	7
3.1 General description of the test site.....	7
3.2 Technical issues about input layers.....	8
3.3 Recharge evaluation	12
3.4 Discussion	20
3.5 Final remarks.....	22
3.6 References	23
4 The Qachqouch aquifer (Case Study Lebanon).....	24
4.1 Study Area: The Qachqouch spring	24
4.2 Methodology.....	25
4.3 Results	29
4.3.1 Individual layer Output	29
4.3.2 Total Recharge and Areal Distribution.....	32
4.4 Discussion and Model Sensitivity	34
4.5 References	36
5 Ubrique test site (case study Spain).....	37
5.1 General description of the test sites	37
5.2 Technical information about input layers	38
5.3 Precipitation.....	40
5.4 Recharge evaluation.....	42
5.5 Discussion and final remarks	45
5.6 References	46
6 The Lez Karst Catchment (case study France)	48
6.1 General description of the test site.....	48
6.2 Technical issues about input layers (GIS)	48
6.3 Recharge evaluation.....	48
6.4 Discussion	49
6.5 Final remarks.....	50
6.6 References	52

7 Hochiften-Gottesacker karst area (test site in Austria).....	52
7.1 Test site	52
7.2 Recharge evaluation.....	53
7.3 References	54
8 Conclusions.....	56
8.1 References	57

1 Introduction

The overarching objective of the KARMA project is to achieve substantial progress in the hydrogeological understanding and sustainable management of karst groundwater resources in the Mediterranean area in terms of water availability and quality. At karst catchment scale, the main objective is to advance and compare transferable modeling tools for improved predictions of climate-change impacts and better-informed water management decisions, and to prepare vulnerability maps as tools for groundwater quality protection.

The main objective of WP2 is the assessment of groundwater availability by investigating recharge, discharge and storage. Recharge consists of the downward flow of rainwater that reaches the water table. Recharge into karst and fissured aquifers can occur in two ways, (1) diffusely over carbonate outcrops, epikarst and soils (autogenic) or (2) from nearby non-karst areas where rainwater infiltrates through swallow holes or dolines (allogenic) (Figure 1.1).

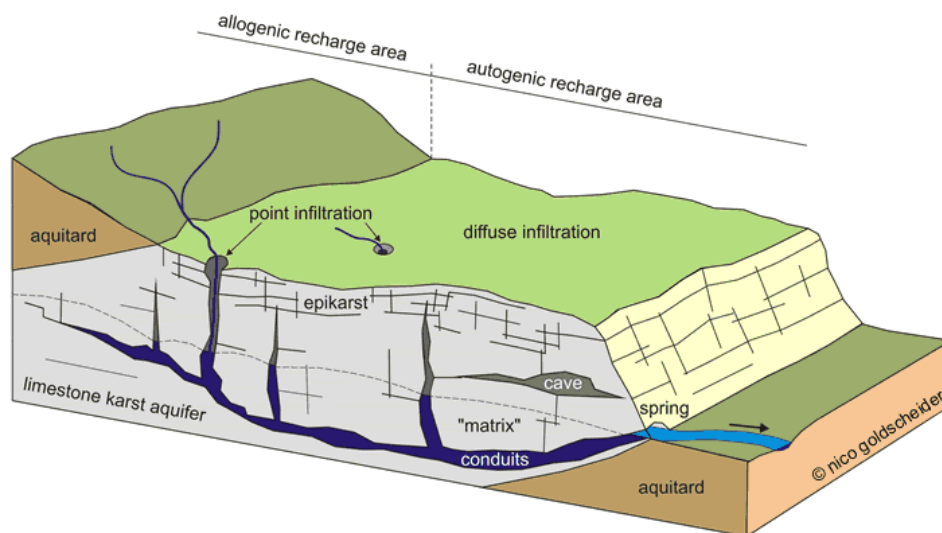


Figure 1.1. Schematic illustration of a heterogeneous karst aquifer system characterized by a duality of recharge (allogenic vs. autogenic), infiltration (point vs. diffuse) and porosity/flow (conduits vs. matrix) (Goldscheider 2019)

The available knowledge about these processes and how infiltration takes place in each KARMA test site highly influences the development of numerical models and vulnerability maps, as well as their accuracy. Therefore, in order to achieve a better hydrogeological understanding and to obtain reliable data for the calibration and validation of models and vulnerability maps, hydrological monitoring, isotope studies, and tracer tests will be carried out in addition to the recharge rate estimation.

When considering an appropriate time scale (decades), it can be assumed that the mean annual value of the recharge is equivalent to the rate of discharge. Thus, groundwater recharge over a defined area is usually equivalent to infiltration excess. Different methods are traditionally applied for groundwater recharge assessment (i.e. hydrological or numerical balance, based on hydrochemistry and environmental isotopes, etc), however none of them are free from uncertainty. Direct determination of recharge from the use of lysimeters and seepage meters, is not always representative for the whole aquifer catchment, neither feasible at such work scale.

2 The APLIS method: general aspects

The APLIS method, originally proposed for a common recharge evaluation within the KARMA project, allows to estimate the mean annual recharge of carbonate aquifers, expressed as a percentage of precipitation. A combination of geological, geographic, morphologic and edaphologic variables, i.e. altitude, slope, lithology, infiltration landforms and soil types (Andreo et al., 2008, Marín, A.I., 2009), are used for the calculation. This GIS-based method was developed from eight well-studied carbonate aquifers in southern Spain, representative of a wide range of climatic and geological systems.

The APLIS method estimates the spatial distribution of the recharge rate within aquifers, according to their particular characteristics and divides it into five classes (Figure 2.1).

Recharge rate (%*)	Class
≤ 20	Very low
20 - 40	Low
40 - 60	Moderate
60 - 80	High
> 80	Very high

(*) In % of the annual mean rain

Figure 2.1. Values of Recharge rates, divided into 5 classes (Andreo et al., 2008).

APLIS estimates the mean annual recharge of carbonate aquifers, expressed as a percentage of the precipitation. Input parameters (Figure 2.2) are: average annual precipitation, its spatial distribution, and a combination of the physical variables that were found to be most influential: altitude (A), slope (P), lithology (L), infiltration landforms (I), and soil type (S). To obtain a map of the average recharge rate, available information about A (altitude), P (slope), L (lithology), I (infiltration landforms), and S (soil) is transformed into dimensionless values from 1 to 10 by a ranking system and subsequently inserted in the following equation:

$$\bar{R}_j = \frac{A_j + P_j + 3L_j + 2I_j + S_j}{0.9} \times F_{hj} \quad \text{Equation 2.1}$$

Where \bar{R}_j is the mean annual recharge rate at a location j, and F_{hj} acts as a correction factor between 0.1 and 1, depending on the permeability of the aquifer. Recharge mapping is fundamental for the appropriate management and protection of karst groundwater resources, in terms of both quantity and quality (Andreo et al., 2008).

Altitude (m) (A)	Rating	Slope (%) (P)	Rating	Soil (S)	Rating	Correction factor (F _n)	Rating
≤300	1	≤ 3	10	Leptosols	10	Aquifer	1
(300–600]	2	(3 - 5]	9	Arenosols and xerosols	9	Other	0.1
(600–900]	3	(5 - 10]	8	Calcareous regosols and fluvisols	6		
(900–1,200]	4	(10 - 15]	7	Euthricregosols and solonchaks	7		
(1,200–1,500]	5	(15 - 20]	6	Cambisols	6		
(1,500–1,800]	6	(20 - 30]	5	Euthriccambisols	5		
(1,800–2,100]	7	(30 - 45]	4	Histosolsandluvisols	4		
(2,100–2,400]	8	(45 - 65]	3	Chromicluvisols	3		
(2,400–2,700]	9	(65 - 100]	2	Planosols	2		
>2,700	10	> 100	1	Vertisols	1		

Lithology (L)	Rating	Infiltration landforms (I)	Rating
Limestones and dolostones karstified	10 or 9	Abundant infiltration landforms	10
Limestones and dolostones fractured, slighted	8 or 7		
Limestones and dolostones fissured	6 or 5	Moderate infiltration landforms	5
Gravels and sands	4		
Conglomerates	3		
Plutonic and metamorphic rocks	2		
Shales, silts, clays	1		

Figure 2.2. Variable scores considered in the APLIS method: Altitude, Slope, Lithology, Infiltration landforms, Soil and Correction factor (Andreo et al., 2008).

3 Gran Sasso aquifer (Case Study Italy)

3.1 General description of the test site

The Gran Sasso hydrostructure is defined as a calcareous-karstic aquifer system of about 1034.4 km² of total extension and is the most representative karst aquifer of the central-southern Apennines. The Gran Sasso hydrogeological system is characterised by Meso-Cenozoic carbonate units (aquifer). It is bounded by terrigenous units represented by Miocene flysch (regional aquiclude) along its northern side, and by Quaternary continental deposits (regional aquitard) along its southern side (Figure 3.1). The system can be divided into hydrogeological complexes each determined by a specific lithology, porosity and permeability (Figure 3.1) which are:

- The complex of recent and ancient continental detrital deposits;
- The complex of recent continental debris units;
- The complex of the ancient continental debris units;
- The complex of marine terrigenous units;
- Marly complex,
- Limestone complex;
- Dolomite complex

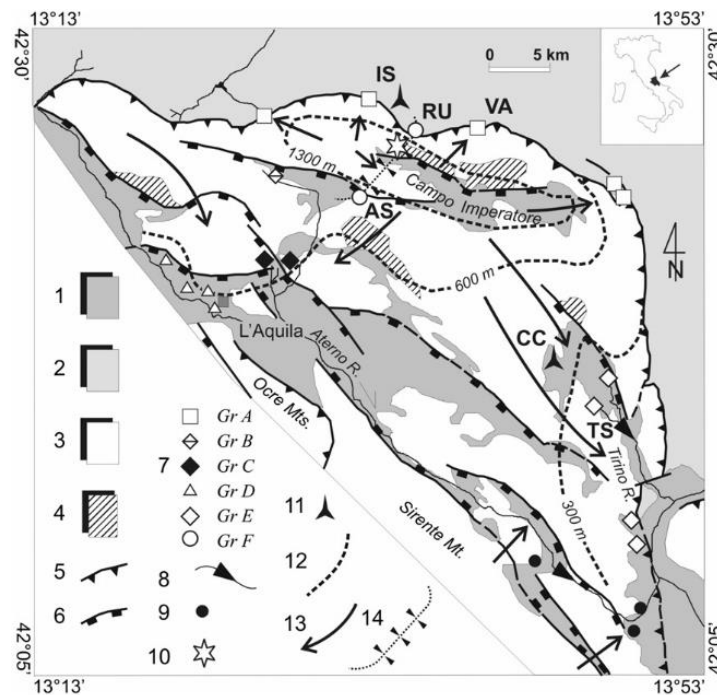


Figure 3.1. Gran Sasso hydrogeological outline. 1: aquitard (continental detrital units of intramontane basins, Quaternary); 2: aquiclude (terrigenous turbidites, Mio-Pliocene); 3: aquifer (calcareous sequences of platform Meso-Cenozoic); 4: low permeability substratum (dolomite, upper Triassic); 5: thrust; 6: extensional fault; 7: main spring: AS: Assergi drainage; RU: Ruzzo drainage; VA: Vacelliera spring; TS: Tirino springs; symbols refer to the six spring groups identified in Barbieri et al. (2005); 8: linear spring; 9: springs belonging to a nearby aquifer; 10: INFN underground laboratories (UL in the text); 11: meteorological station (IS: Isola Gran Sasso, CC: Carapelle Calvisio); 12: presumed water table in m asl; 13: main groundwater flow path; 14: highway tunnels drainage. [Amoruso, 2012]

The Gran Sasso karst aquifer hosts a unique regional-wide groundwater table. The main springs have been classified into six groups based on groundwater flow and hydrochemical characteristics, as illustrated in Figure 3.1. The aquifer has a total discharge of more than 18 m³/s from its springs (Amoruso et al., 2012), including a highway tunnel drainage tapped for drinking water on both sides. The massif's core, an endorheic basin having tectonic-karst origin, called Campo Imperatore basin (elevation 1650 m a.s.l.), acts as preferential recharge area of the Gran Sasso aquifer, fed by high rainfall and snowfall. On the massif of the Gran Sasso, it is possible to recognize numerous superficial karst morphologies widespread on the southern slope, where there are numerous locally closed depressions. These are flat-bottomed endorheic depressions, classifiable as *polje*. This type of morphology constitutes very large areas of widespread infiltration, deep underground tunnels, and karst canals.

A complete description of the aquifer characteristics is available in D2.1 (Preliminary Water Budget). In this document additional details on groundwater flow characteristics are included, coupled with a detailed evaluation of the water budget.

3.2 Technical issues about input layers

For the Gran Sasso site, maps of the above variables have been drawn, using a geographic information system (GIS). The software arcGis 10.3 (Esri) has been used with a referencing system of WGS 1984 UTM Zone 33N. The analysed area extends about 1034 km² and the adopted cell size is 20 m x 20 m. For the realisation of the all-variables map, the “*Workshop on groundwater recharge assessment in carbonate (karst) aquifers by APLIS method*” guide, created by Ana I. Marín, Juan Antonio Barberá and Jaime Fernández-Ortega (2020) has been considered, following it step by step.

In detail, the altitude map was derived from the digital elevation model (DEM), produced by the Department of Structural, Water and Soil Engineering of L'Aquila University, by Prof. Marco Tallini and his team, using a cell size of 20 m x 20 m. The altitude of the considered area ranges from a maximum altitude of 2900 m a.s.l. to the lowest elevation that corresponds to 300 m a.s.l.

Considering the table of various scores, the altitude map was reclassified using the values of the *Altitude* table as a reference, as illustrated in the Figure 3.2. The percentage of pixels in the different altitude classes of the site under examination was also reported.

With the same data, the slope map of the study area has been realized. The map of slopes was created based on the DEM, in ArcGIS 10.3, plotting a triangulated irregular network corresponding to homogeneous areas of the different slope intervals (Figure 3.3). For each cell, the Slope tool calculates the maximum rate of change in value from that cell to its neighbors. The maximum value is shown mainly in the northern area, in correspondence to high-altitude areas.

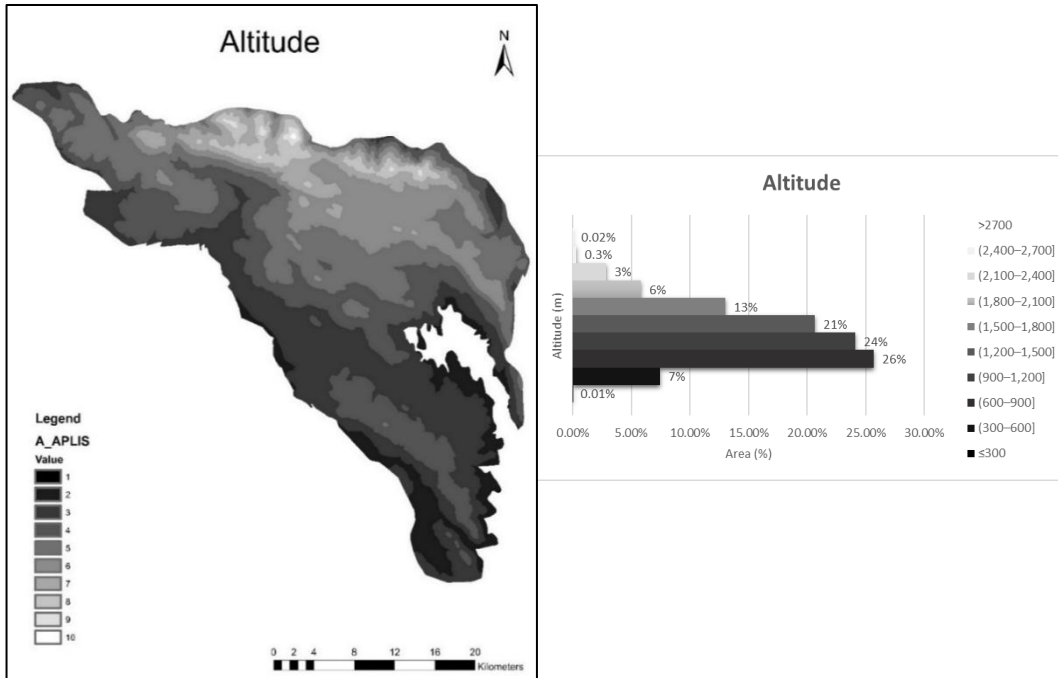


Figure 3.2. Altitude map derived from Digital Elevation Model (DEM) with a resolution of 20x20 m cell size. The highest percentage of altitude is in the 3rd class, with a range from 600 m to 900 m.

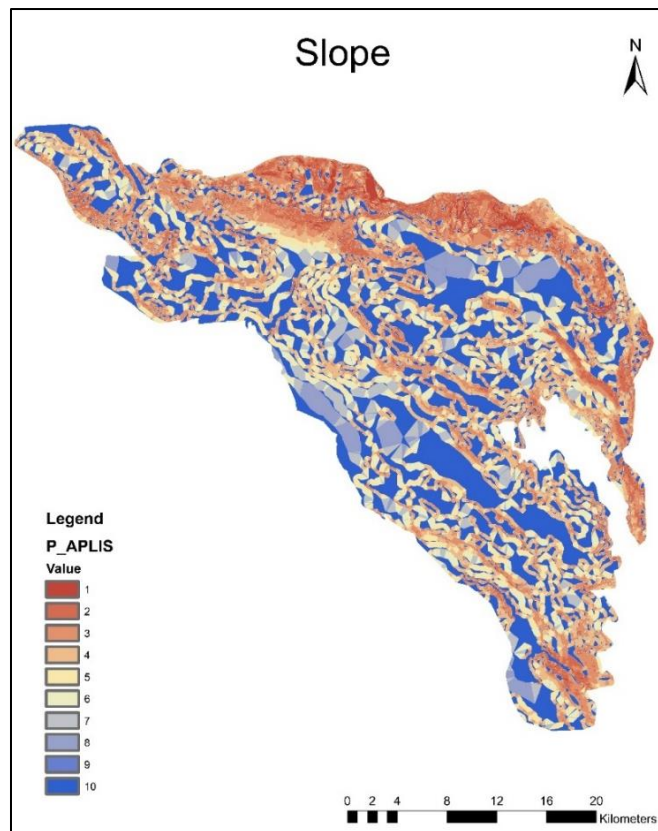


Figure 3.3. Slope map created with the arcGis software.

For the Lithology variable (L), the geological map derived from the “*Schema idrogeologico del massiccio del Gran Sasso*” (Petitta et al., 2002) with a scale of 1:150.000 has been considered, tacking also into account the characteristics of hydrogeological complexes described in Farroni et al., 1999.

Subsequently, the right score was determined based on the lithology and the table in Figure 2.2.

The lithologies outcropping in the Gran Sasso hydrogeological basin summarized as hydrogeological units are:

- Dolomitic Complex;
- Limestone Complex;
- Limestone-Marly Complex;
- Terrigenous Units;
- Detrital Units.

Different scores have been given to the different types of lithologies based mainly on their fracturing and karstification, always taking the initial table as a reference. The lithology ranges from a calcareous complex with a score of 10 to a terrigenous complex with a score of 2. The calcareous complex is characterised by a very high permeability, especially due to fracturing and karstification. This complex constitutes the main aquifer of the Gran Sasso hydrostructure, where the regional base water table is located. The effective infiltration is very high and there is practically no surface runoff, in addition, it represents one of the main aquifer recharge areas. The terrigenous complex, on the other hand, constitutes the main limit of the regional aquifer, acting as an aquiclude whose permeability through porosity is very low (Farroni, 1999).

In detail, the scores given to the different lithologies and the corresponding map created with the GIS software are shown in Figure 3.4.

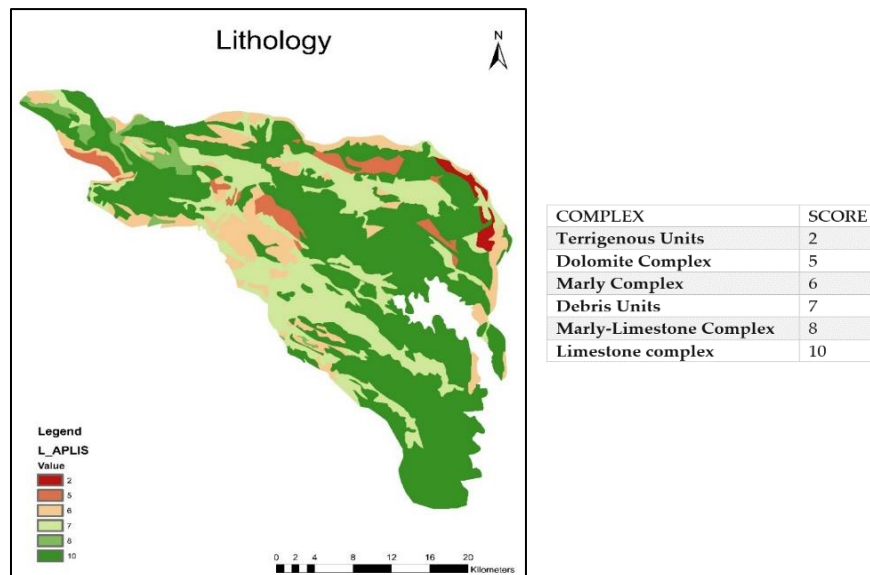


Figure 3.4. Lithology map with Table attribute of the different type of lithologies outcrop in the study site.

Areas of preferential infiltration were derived from the geomorphological map, annexed to the *Piano Stralcio di Bacino per l'Assetto Idrogeologico dei Bacini Abruzzesi* ("Gravitational phenomena and erosive processes", 2017). It identifies the shapes based on the dominant morphogenetic agent and represents them using the conventional colours. Regarding karst morphologies, dolines and karst swallow holes have been identified in the Gran Sasso area (Figure 3.5).

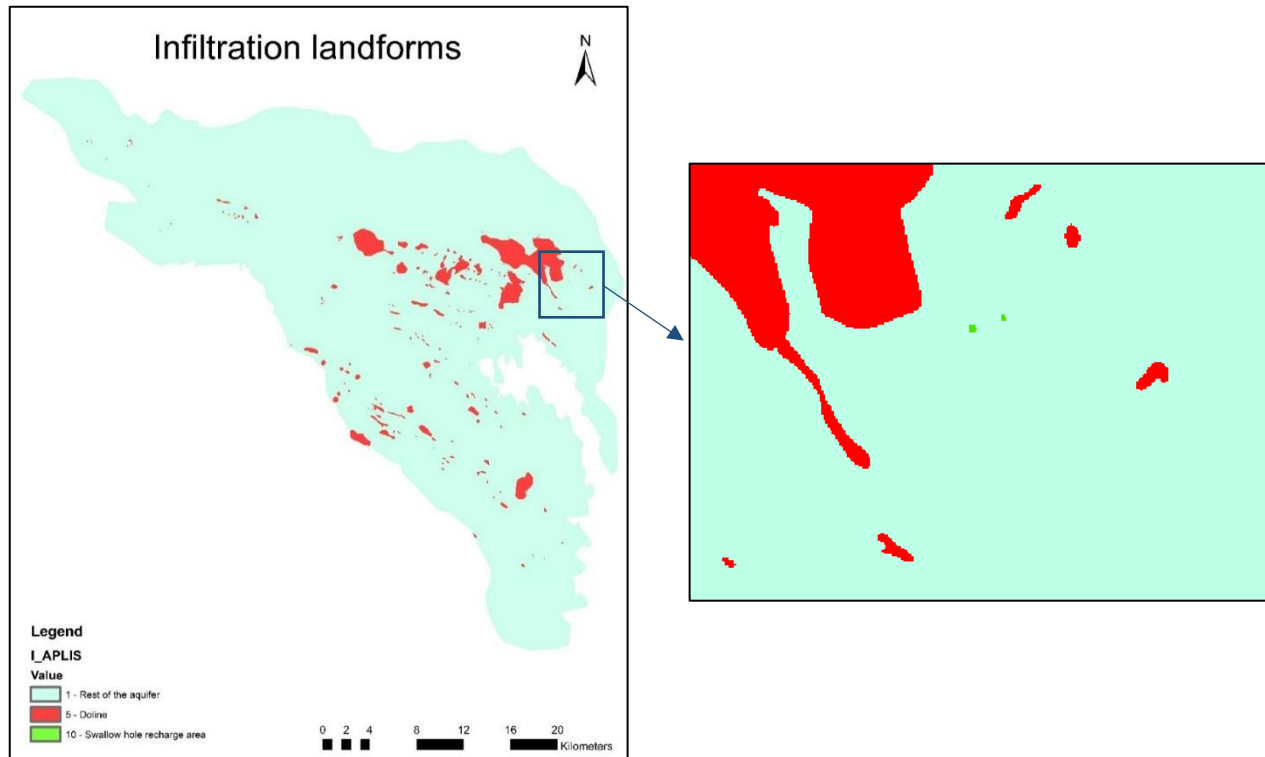


Figure 3.5. Infiltration landform map (left). Detailed view of the swallow holes (right).

Finally, the soil map was derived from the geoportal of the Abruzzo region. The main geometric reference from which the land use limits were taken was represented by the 1997 AIMA digital orthophoto (scale 1:10000) and Landsat TM5 satellite images (30x30 meters pixels), acquired in three steps corresponding to late spring, summer, and winter to cover significant phenological phases of natural vegetation and main agricultural crops.

The main soil types, as shown in the Figure 3.6, are Luvisol, Euthric cambisol, Cambisol and Leptosol, to whom a score of 4, 5, 6 and 10 have been assigned.

Finally, F_h was calculated. F_h corresponds with the recharge correction factor (R), which is expressed as a percentage of precipitation. The F_h factor depends on the hydrogeological characteristics of the materials outcropping on the surface. According to the APLIS classification, values of 1 are applied where aquifer outcrops, while other parts are indicated by value of 0.1.

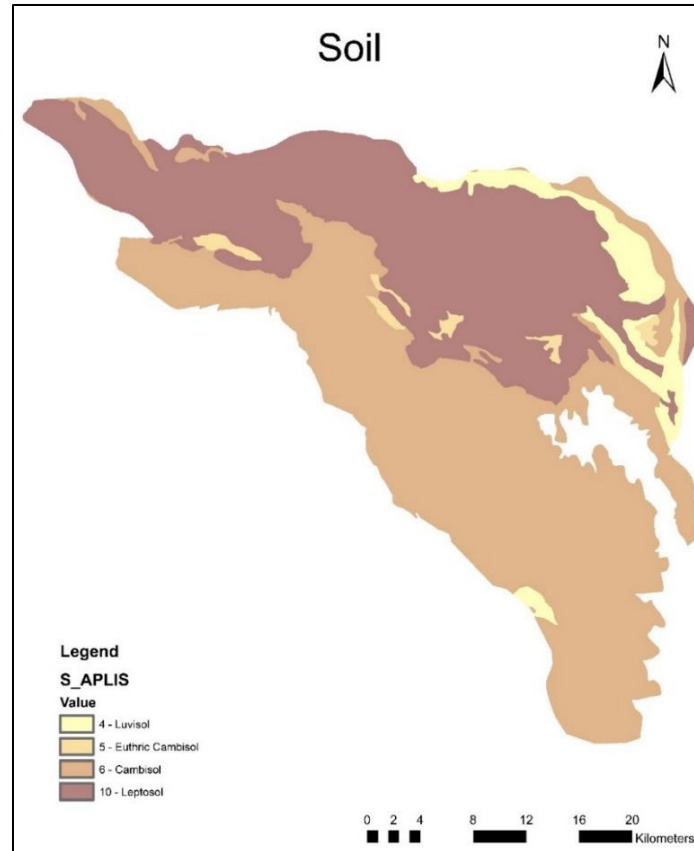


Figure 3.6. Soil map.

3.3 Recharge evaluation

From the above described variables map, a combinatory procedure has been applied to produce a single calculation algorithm enabling one to determine the known recharge value and the spatial distribution of recharge rate within the Gran Sasso karst aquifer. In fact, as well as calculating the recharge rate, the APLIS method enables us to obtain maps the spatial distribution by the superimposition of the information layers in the GIS software (Figure 3.7).

The equation used and calculated with the GIS software in order to have a recharge value on the aquifer considered is:

$$R = [(A + P + 3xL + 2xI + S) / 0,9] \cdot Fh$$

The weight of each variable in the above expression is intended to represent its relevance in determining the recharge rate. The lithology variable has three times as much influence as those of altitude, slope, and soil type, while areas of preferential infiltration are twice as important. The mean value of the annual recharge rate is grouped into five regular intervals, each of which is assigned to a recharge class (TABLE): very low, low, moderate, high, very high. The final recharge map obtained by APLIS is shown in Figure 3.7.

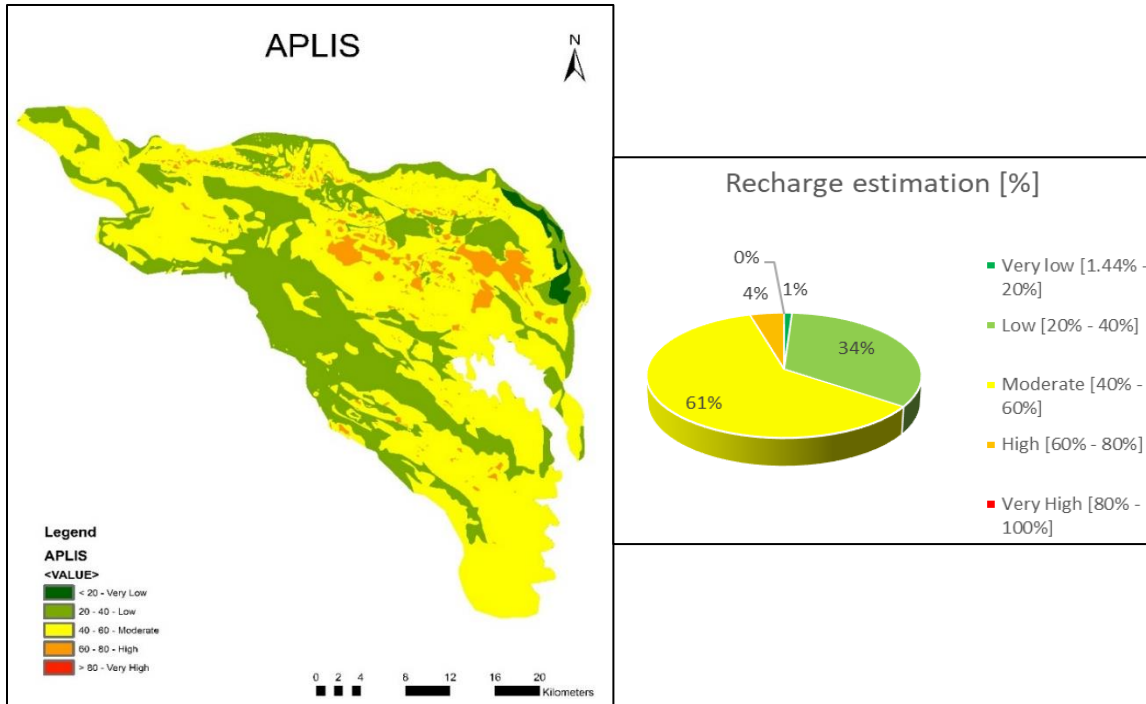


Figure 3.7. Recharge map (%) of the Gran Sasso aquifer obtained by APLIS method.

Most of the infiltration percentages are grouped into the categories low (20-40%) and moderate (40-60%). Of the total permeable surface, 61% is moderately recharged, while the 34% is characterised by low recharge. Areas with high infiltration are characterized by the presence of dolines and swallow holes, but there is also the area of Campo Imperatore, identified as the preferential recharge area. The average value of effective infiltration in the Gran Sasso aquifer is 50.6%. The recharge rate is conditioned by the higher altitude and the development of infiltration forms.

With the software GIS it is also possible to define maximum, minimum and mean values of recharge in the studied area. It has been observed that the maximum value of recharge in the Gran Sasso aquifer is 73.33%, while the minimum value of recharge is 1.77% (Figure 3.8).

Statistics	
Band_1	
Build Parameters	skipped columns:1, rows:1, ignored value(s):
Min	1.777777791023254
Max	73.33333587646484
Mean	50.57543851559293

Figure 3.8. The minimum, maximum and mean values of the recharge map created with APLIS method.

Additionally, overlaying this APLIS layer with a raster that contains precipitation values, it is possible to estimate the quantity of water that recharges the aquifer through direct infiltration. For this reason,

precipitation was estimated by creating and mapping isohyets, initially examining 21 thermo-pluviometric stations in the Gran Sasso area. The data from the thermo-pluvial stations were requested to the hydrographic service of the Abruzzo Region, for the period 2000-2020. Their positions are shown in Figure 3.9. Unfortunately, most of the analysed thermo-pluviometric stations are affected by data gaps.

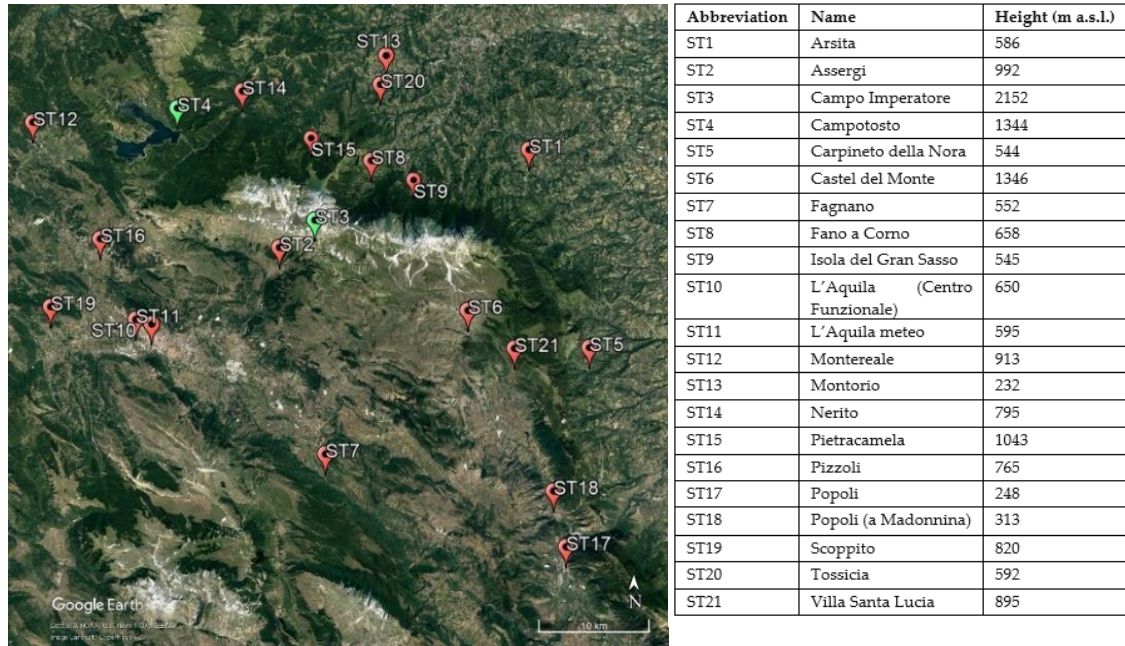


Figure 3.9. Location of the thermo-pluviometric station in the Gran Sasso area. Red symbols show the thermo-pluviometric stations, while green symbols show the thermo-pluviometric with additional snow stations. In the table on the right, abbreviation, name and height of each station are listed.

For the realisation of the isohyet maps, the article of Scozzavafa and Tallini (2001) was taken as a reference, in which two annual rainfall gradients for the northern and the southern side of the massif, were used. Following the authors methodology and based on 20 years of climate data monitoring (2000-2020), two annual rainfall gradients were calculated. Specifically, the gradient was found by correlating altitude and precipitation values of the different thermo-pluviometric stations located in the northern and southern part of Gran Sasso massif. In particular, for the southern side the calculated gradient is 30/100 m obtained by the following equation:

$$P = 0.3H + \text{precipitation annual value of the south station}$$

while for the northern side the calculated gradient is 42/100 m gained from the equation:

$$P = 0.42H + \text{precipitation annual value of the north station}$$

where P is the calculated precipitation values for each cell of the grid and H is the altitude.

The stations of Campotosto (1344 m a.s.l.) for the Northern side and the station of Assergi (992 m a.s.l.) for the Southern side were taken as representative (Figure 3.10). The annual precipitation values of the thermo-pluviometric stations Assergi and Campotosto in the period from 2000 to 2020 are shown below.

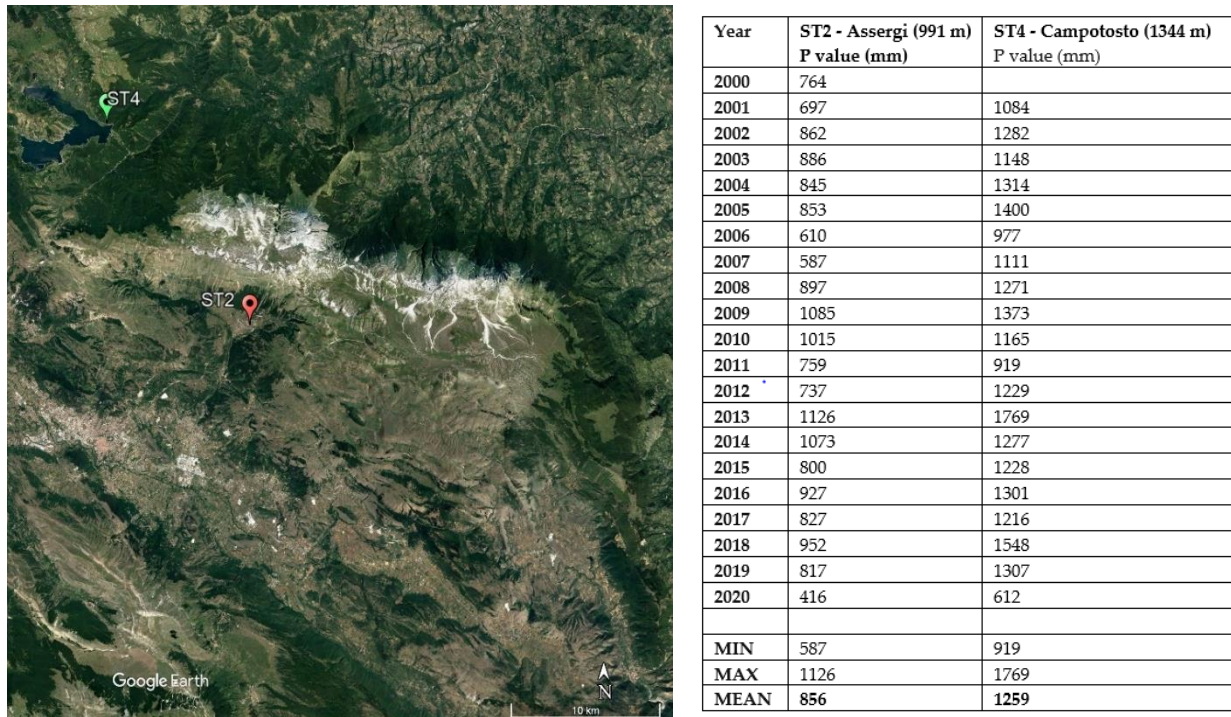


Figure 3.10. Location of the two thermo-pluviometric stations considered for the map of isohyets (Campotosto in green and Assergi in red). In the Table beside the precipitation values of Assergi and Campotosto stations in the period 2000-2020 have been reported.

Starting from the benchmark values of mean precipitation for the long monitoring period 2000-2020 (856 mm for Assergi and 1259 mm for Campotosto), the isohyet map was created.

Taking the altitude of the two stations and the above-mentioned average precipitation values into consideration, the isohyet map was created using a gradient of 30/100 m for the southern side and 42/100 m for the northern side, according with the methodology proposed in Tallini (2001) and Farroni (1999). Due to the wide extension of the hydrogeological basin (1034 km²), a cell size of 100 m x 100 m was used for the calculation of precipitation values to simplify the computing operation with arcGis. To create isohyet curves, Contour tools with an interval of 100 mm have been used.

For the considered interval time (2000-2020) the precipitation values, shown in Figure 3.11, range between 646 mm to 1931 mm. Precipitation values obviously increase with altitude and the maximum values are reached at the mountain peaks (e.i. Gran Sasso reaches up to 2900 mm).

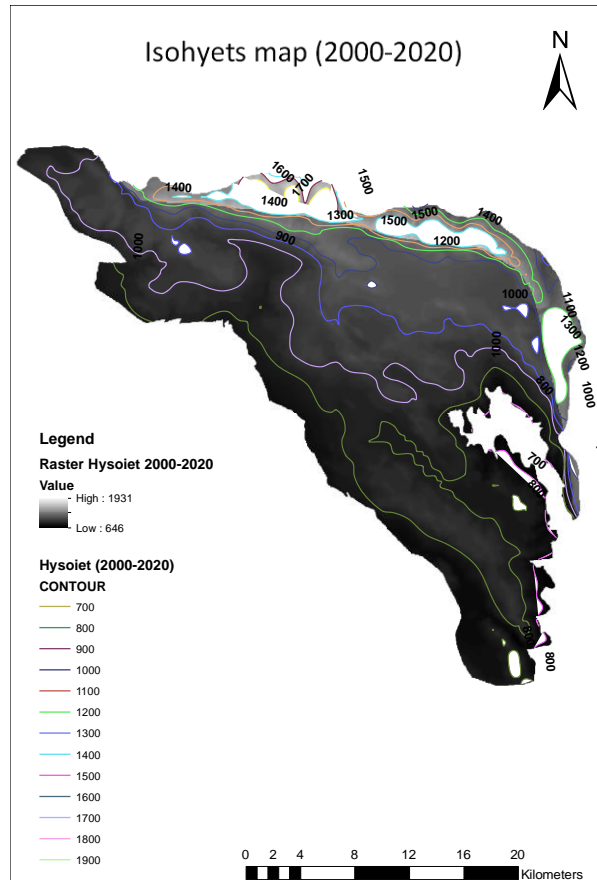


Figure 3.11. Isohyets map (2000-2020) created using ArcGis.

The calculated isohyet map, plotted on a 20x20 m raster from a 100x100 m raster, was combined with the APLIS map (Figure 3.7), to derive the infiltration and recharge of the aquifer. As shown in Figure 3.12, the infiltration values range from 19 mm to 1259 mm. The calculated mean value of the long-term infiltration is 484 mm. The recharge in the Gran Sasso hydrogeological basin obtained through APLIS is 15.9 m³/s, about 10% lower than the measured mean recharge in the entire aquifer (Amoruso et al., 2012; considering the period 1999-2009).

Aquifer recharge can be also determined using conventional methods such as hydrodynamic or hydrological balance calculations. With this type of methods only some of the components in the groundwater budget equation can be measured directly (for example precipitation data), while the rest (i.e. potential and real evapotranspiration, effective rainfall) must be estimated indirectly using a semi-empirical formula proposed by Thornthwaite (1948), and Turc (1954).

The Gran Sasso aquifer has been studied in detail over the last 15 years and different methodologies have been applied to determine the effective infiltration. In particular, Scozzafava and Tallini (2001) provide a partly modified application of the Thornthwaite method, while Boni et al. (1986) proposed a method of "direct" evaluation of the effective infiltration. Both methodologies and results are precisely described in D2.1 (Preliminary Water Budget).

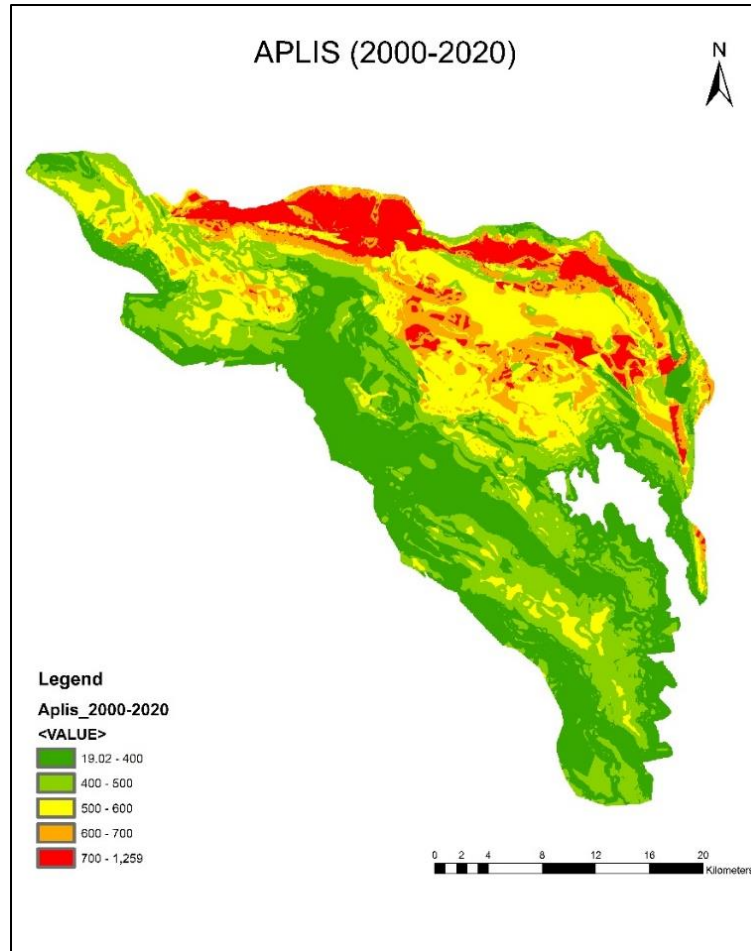


Figure 3.12. Infiltration map overlaying the APLIS map of the test site and the map of the precipitation of the period 2000-2020.

Based on the knowledge of the hydrogeological system, the Turc method (1954) for the estimation of ETR at annual scale was applied in order to assess the infiltration values and to calculate an updated water balance for the study area. The Turc-equation to calculate ETR is:

$$ETR = \frac{P}{\sqrt{0.9 + \frac{P^2}{L^2}}}$$

where P is the mean value of the precipitation and L is:

$$L = 300 + 15T + 0.05T^3$$

With T being the temperatures mean value.

The ETR estimation with the Turc-method was applied, as for the APLIS method, to the monitoring period 2000-2020. As shown in the equations, it is necessary to define precipitation and temperature distribution on the hydrogeological basin at first.

Therefore, temperature values have been determined (T), taking the precipitation distribution previously calculated for the application of APLIS method into account (Figure 2.11). Based on the methodology applied for the calculation of the rainfall gradient, an estimation of the temperature gradient was computed. In this case, only one gradient value was adopted for the entire area and temperature values were obtained using the following equation:

$$T = -0.59H + \text{average temperature of the reference station.}$$

The adopted representative site is Castel del Monte thermo-pluviometric station (altitude: 1346 m a.s.l., shown in Figure 3.13). Starting from the computed T values calculated for each cell (100 m x100 m resolution) an isotherm-map for the 2000-2020 monitoring period was drawn, using the Contour tool with an interval of 2 °C (Fig. 3.14).

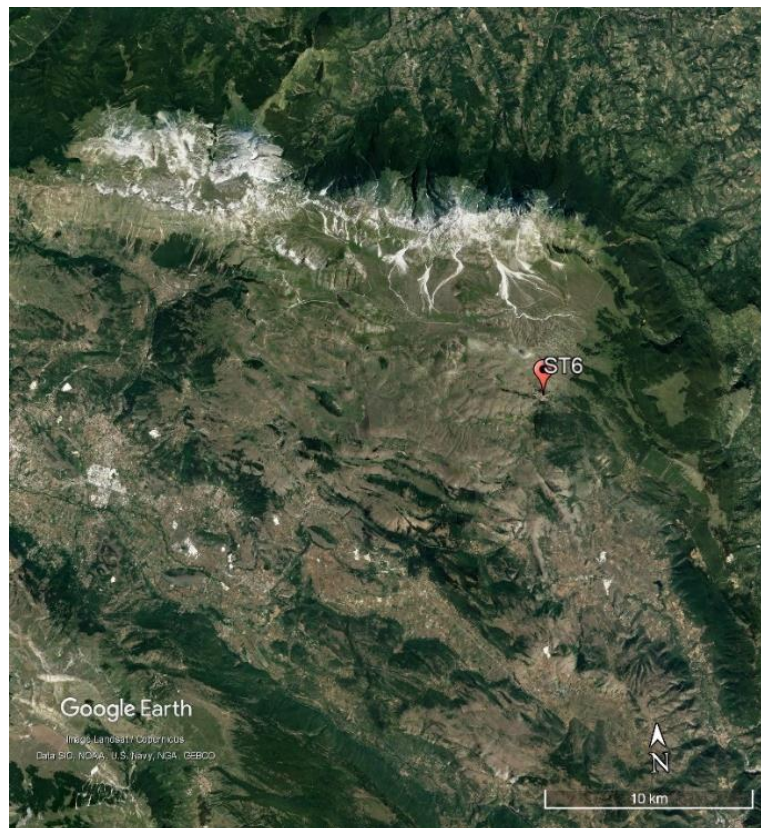


Figure 3.13. Location of the Castel del Monte thermo-pluviometric station used for the realisation of the isotherms map.

The monitored years were also treated individually applying the Thornthwaite method for the estimation of ETR at a monthly scale. In particular, the years 2002 and 2016 have been analysed; 2002 has been selected because it is the year in which the average annual precipitation value is very close to the long-term (2000-2020) average precipitation value on the massif, while 2016 was considered to evaluate the contribution of snow on the water balance.

In Table 3.1 the rainfall values from 2002 and 2016 of the two considered stations are shown and compared with the mean precipitation value for the long period (2000-2020).

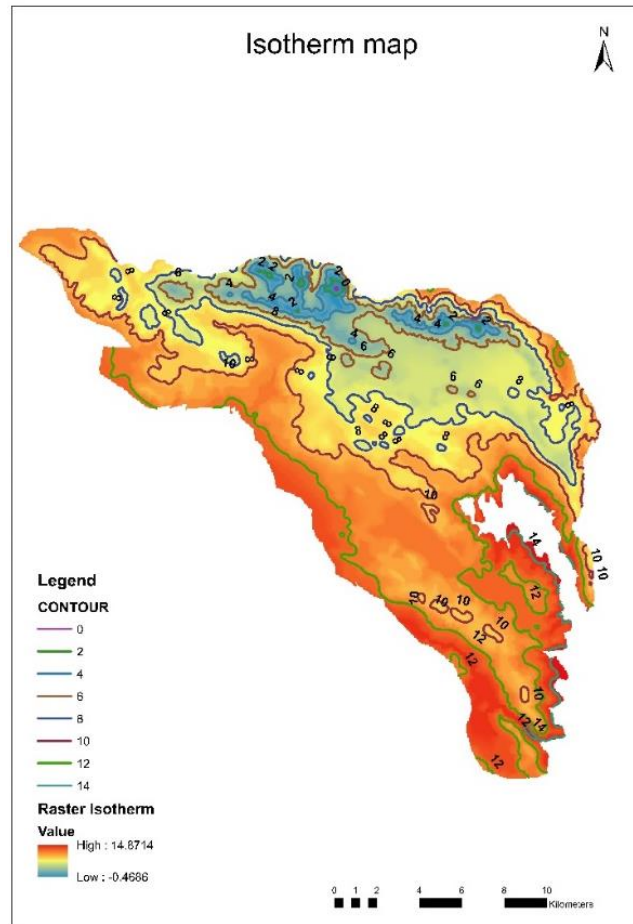


Figure 3.14. Isotherm map of the Gran Sasso aquifer for the period 2000-2020.

Table 3.1. Precipitation data of the years 2002 and 2016 of the considered stations and the mean value for the long period 2000-2020.

Year	ST2 - Assergi (991 m) Precipitation (mm)	ST4 - Campotosto (1344 m) Precipitation (mm)
2002	862	1282
2016	927	1301
MEAN (2000-2020)	856	1259

To obtain a monthly estimation of ETR and consequently the net infiltration, precipitation values for each month of the chosen year were calculated starting from the average precipitation values of the two reference stations, one for the northern (Campotosto) and one for the southern side (Assergi).

To do this, monthly rainfall gradients (Scozzafava and Tallini, 2001) have been calculated for each side using the annual rainfall gradient:

$$Gm_i = \frac{Rm_i}{Ra_i} Ga_i$$

where $i=1, \dots, 12$ (month), G_{mi} is the monthly rainfall gradient and the unknown variable, G_{ai} is the annual rainfall gradient, R_{mi} is the monthly rainfall, and R_{ai} is the annual rainfall (Scozzafava and Tallini, 2001). Data to apply Thornthwaite's method has been elaborated obtaining the different parameters useful to determine the infiltration value (such as ETP, ETR, field capacity). The field capacity value was obtained through the curve numbers (CN) determined by Scozzafava and Tallini (2001), where for each curve number the ST value is associated. The ST is the maximum water storage in the soil that we adopted as field capacity values.

Moreover, according to Scozzafava and Tallini (2001), the runoff value is about 0.29% of the total precipitation in the considered year.

As mentioned above, for 2016 an attempt was made to analyse the snow data through a gradient of 0.24/100 m that was also calculated by Fazzini and Bisci (1999). The only usable and reliable snow station in the examined area is Campo Imperatore (altitude 2152 m a.s.l.). Additionally, the snowfall contribution to infiltration was estimated using the gradient of 0.24/100 m.

3.4 Discussion

In this paragraph a detailed overview and a comparison between results obtained by the application of different methodologies is given. Specifically, an estimation of infiltration (net of ETR and runoff) and consequently discharge have been carried out for the Gran Sasso site, using APLIS and the methods from Turc and Thornthwaite, for a long-time monitoring period (2000-2020) and also for 2002 and 2016. For the long-time monitoring period (2000-2020), the infiltration values calculated with APLIS and Turc's method are very similar: 484 mm/y with the APLIS method and 515 mm/y with Turc's method, showing a discrepancy of about 6% (Table 3.2). These values are also similar to the net infiltration value calculated by Scozzafava & Tallini (2001) using the Thornthwaite + CN method (506 mm/y).

Table 3.2. Infiltration values for the period 2000-2020 calculated with the method from Turc (1954) and APLIS.

TURC	2000-2020		APLIS	2000-2020
P mean	954.1 mm		Infiltration	484 mm
T mean	9.6 °C		Discharge	15.87 m ³ /s
ETR	436 mm			
Rainfall	2.76 mm			
Infiltration	515 mm			
Discharge	17 m ³ /s			

Moreover, the recharge values for the Gran Sasso karst aquifers calculated with APLIS are similar to those previously calculated with conventional methods and are confirmed by discharge values, with a discrepancy of about 10%, which corroborates the applicability of the method.

The comparison between input and output discharge (measured at springs) of the Gran Sasso aquifer shows a possible underestimation of the recharge. Considering the comparable results obtained by different methods, this underestimation has been attributed to the lack of evaluation of the snowpack and snowmelt to the infiltration in karst outcrops. For this reason, an attempt to evaluate this possible contribution has been carried out. As mentioned above, we tested this evaluation for 2016, because an analysis of the snowpack coverage using aerial and satellite photos was carried out in the framework of a master thesis (Matani, 2016). For the winter of 2016, the additional recharge based on the snowmelt is limited to about 0.5 m³/s for the whole aquifer, which seems to be a negligible component of the water balance, corresponding to only about 3% of the water budget. Undoubtedly, additional efforts need to be applied for a more reliable evaluation of the contribution of snow to the aquifer recharge; we are still working on this question.

The infiltration values for 2002 and 2016 obtained by the application of Turc, Thornthwaite, and APLIS are shown in Table 3.3. In both years the infiltration value derived by the APLIS method is slightly higher than the ones derived by Turc and Thornthwaite, but all results show a general agreement within the different applied methods. Data differ of about 6%, confirming the reliability of the approaches in balance evaluation.

Table 3.3. Infiltration values of 2002 and 2016 derived from the application of the three different methodologies: Turc (1954), Thornthwaite (1948) and APLIS. T mean modified is the temperature value calculated with the Thornthwaite method without negative values.

TURC	2002		Thornthwaite	2002	APLIS	2002
P mean	962 mm		P mean	962 mm	Infiltration	488 mm
T mean	9.7 °C		T mean real	9.7 °C	Discharge	16.07 m3/s
ETR	529 mm		T mean modified	10.79 °C		
Runoff	2.79 mm		ETR	583.2 mm		
Infiltration	429 mm		Runoff	2.79 mm		
Discharge	14 m3/s		Infiltration	450.48 mm		
			Discharge	14.7 m3/s		
TURC	2016		Thornthwaite	2016	APLIS	2016
P mean	1022 mm		P mean	1022 mm		
T mean	8.8 °C		T mean real	8.8 °C	Infiltration	518.5 mm
ETR	529.86 mm		T mean modified	9.8 °C	Discharge	17 m3/s
Runoff	2.96 mm		ETR	605.5 mm		
Infiltration	488.77 mm		Runoff	2.98 mm		
Discharge	16.02 m3/s		Infiltration	483.67 mm		
			Discharge	15.86 m3/s		

Moreover, an infiltration map, overlapping the precipitation map to the APLIS map, has been created, both for 2002 and 2016, as shown in Figure 3.15.

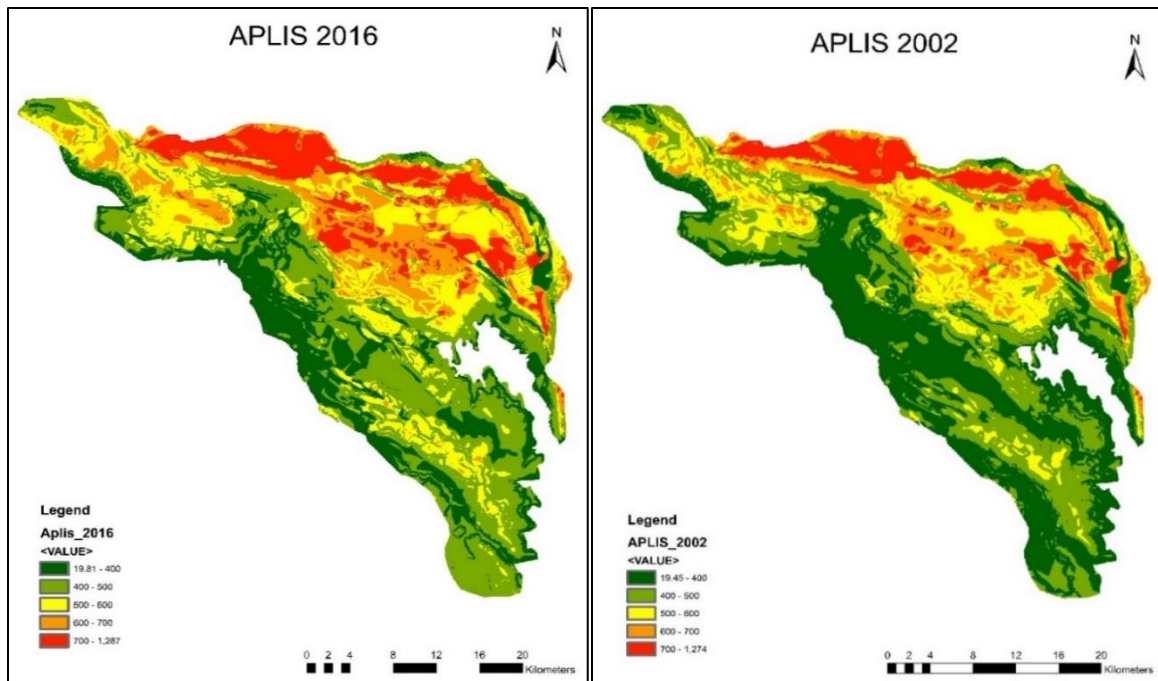


Figure 3.15. Infiltration map of 2002 and 2016 using APLIS.

3.5 Final remarks

For the Gran Sasso aquifer, the previously released water budgets, applying indirect methods, represent a relevant basis of knowledge. The methodology applied by Scozzafava & Tallini (2001) to determine the effective infiltration of the Gran Sasso aquifer, provides input for the application of the Thornthwaite method (Thornthwaite & Mather, 1957), modified according to local hydrogeological characteristics. The Thornthwaite method has been modified to discriminate between runoff and net infiltration by applying the soil Curve Numbers for different recharge areas inside the aquifer.

Starting from the bibliographic data, net infiltration (net of ETR and runoff) was analysed using three different approaches: Evaluation of Evapotranspiration by Turc, Thornthwaite, and APLIS.

In detail, three time periods were taken: a long period 2000-2020 and two single years (2002 and 2016). For each period, obtained infiltration values were found to be very similar to each other and also similar to literature values, showing a slight underestimation of the aquifer discharge values. This can obviously indicate how much and how reliable the three methods can be for studying the balance of the site of interest. The results obtained show infiltration values from 429 mm (with Turc) to 450 (with Thornthwaite) to 488 mm (with APLIS) for 2002. A similar result can also be observed for 2016, ranging from a value of 483 mm (with Thornthwaite) to 488 mm (with Turc) to a value of 518.5 mm (with APLIS). The infiltration values, and therefore also the discharge values, are higher for the year 2016 because of higher rainfall compared to 2002, ranging from 962 mm to 1022 mm in 2016. The obtained values have also been compared with the results of the discharge. Moreover, the infiltration values obtained for the long period 2000-2020 by the Turc method, about 515 mm, correspond to the above cited values of 2002 and 2016 and they are, as shown, very comparable data.

We considered the underestimation of the obtained discharge by a comparison with the calculated recharge values, as due to an evaluation lack of the snow melting component in the hydrological balance, with particular reference to Campo Imperatore endorheic basin. Obviously in karst mountainous areas, where snowmelt is crucial for the infiltration component, this contribution during snowmelt periods, has to be evaluated. This parameter impacts the areal distribution and amount of aquifer recharge over time. In high-altitude areas, recharge would be negligible or sporadic during snowfall periods, because precipitation is in a solid form and the snow and ice cover hinders recharge. The first attempts to include the snow recharge show a limited contribution to the discharge of about 3%, which still seems underestimated with respect to the real influence of this parameter, as confirmed by the comparison with discharge data. Additional efforts will be done to reach a satisfactory agreement between recharge and discharge by a more reliable evaluation of snow cover effects.

3.6 References

- Amoruso, A., Crescentini, L., Petitta, M., & Tallini, M. (2013). Parsimonious recharge/discharge modeling in carbonate fractured aquifers: The groundwater flow in the Gran Sasso aquifer (Central Italy). *Journal of Hydrology*, 476, 136–146
- Andreo B., Vias J., Duran J., Jimenez P., Lopez-Geta J.A., Carrasco F. (2008). Methodology for groundwater recharge assessment in carbonate aquifers: application to pilot sites in southern Spain. *Hydrogeology Journal* 16, 911-925
- Boni C., Bono P., Capelli G. (1986). Schema idrogeologico dell'Italia centrale. *Mem. Soc. Geol. It.*, 35, 991-1012, 2 tav., Roma.
- Fazzini M., Bisci C., (1999). Clima e neve sul massiccio del Gran Sasso. *Neve e Valanghe*, Vol. 36
- Marin I.A., Barbera J.A., Fernandez-Ortega J. (2020)- Workshop on groundwater recharge assessment in carbonate (karst) aquifers by APLIS method
- Petitta, M., & Tallini, M. (2002). Idrodinamica sotterranea del massiccio del Gran Sasso (Abruzzo): Nuove indagini idrologiche, idrogeologiche e idrochimiche (1994-2001). *Bollettino Della Società Geologica Italiana*, 121(3), 343–363.
- Scozzafava, M., & Tallini, M. (2001). Net infiltration in the Gran Sasso Massif of central Italy using the Thornthwaite water budget and curve-number method. *Hydrogeology Journal*, 9(5), 461–475.
- Tallini, M., Petitta, M., Ranalli, D. (2000). Caratterizzazione chimico-fisica e idrologica delle acque sotterranee del massiccio del Gran Sasso d'Italia (Italia centrale): Analisi statistica dei dati esistenti. Dipartimento di Ingegneria delle Strutture, delle Acque e del Terreno, Aquila. DISAT.
- Thornthwaite, C. W. (1948). An approach toward a rational classification of climate. *Geographical review*, 38(1), 55-94.
- Thornthwaite, C.W. and Mather, J.R., (1957). Instructions and tables for computing potential evapotranspiration and the water balance. *Publ. Climatol.*, 10(3).
- Turc, L. 1954 Calcul du bilan de l'eau: evaluation en fonction des precipitations et des temperatures. *Int. Assoc. Sci. Hydrol.* 38(3), 188–202

4 The Qachqouch aquifer (Case Study Lebanon)

4.1 Study Area: The Qachqouch spring

Qachqouch Spring (Figure 4.1), is located within the Nahr el Kalb Catchment and originates from the Jurassic karst aquifer at about 64 meters above sea level. During low flow periods, the spring is used to complement the water deficit in the capital city Beirut and surrounding areas. Its total yearly discharge reaches 35-55 Mm³ based on high-resolution monitoring of the spring (2014-2019; Dubois et al., 2020). Flow maxima reach a value of 10 m³/s for a short period following flood events; discharge is about 2 m³/s during high flow periods and 0.2 m³/s during recession periods.

About 67% of the area in Lebanon consists of karstified (6,900 km²) rock sequences (Dubois, 2017). The catchment area drained by the Qachqouch spring is delimited to the North by Nahr El Kalb River and extends for more than 55 km² of mountainous nature at a maximum elevation of 1650 m.a.s.l. (Dubois, 2017). Tracer experiments show a relationship between the Nahr El Kalb River and the Qachqouch Spring through a sinking stream (Doummar and Aoun, 2018b).

The spring originates from a carbonate aquifer composed of the Jurassic formation sequence of massive fissured limestone of more than 100 m in thickness. Dolostones characterized by a higher porosity (10-12%) are found in the lower part of the formation because of the diagenetic dolomitization and along leaky faults and dykes because of hydrothermal dolomitization (Nader et al., 2004). The investigated area is located in the tectonic regime of a major fault, Yammouneh Fault, causing tectonic deformation and fracturing of the catchment area. Multi-level karstification in the Mediterranean was developed during the Messinian salinity crisis and Quaternary glacial events causing deep karst systems with features such as large dissolution conduits, dolines, sinkholes, and caves (Bakalowicz, 2015; Dubois et al., 2020). The area is characterized by a duality of infiltration portrayed by the point source infiltration in preferential pathways (dolines, permeable faults) and diffuse recharge in bare fissured rocks.

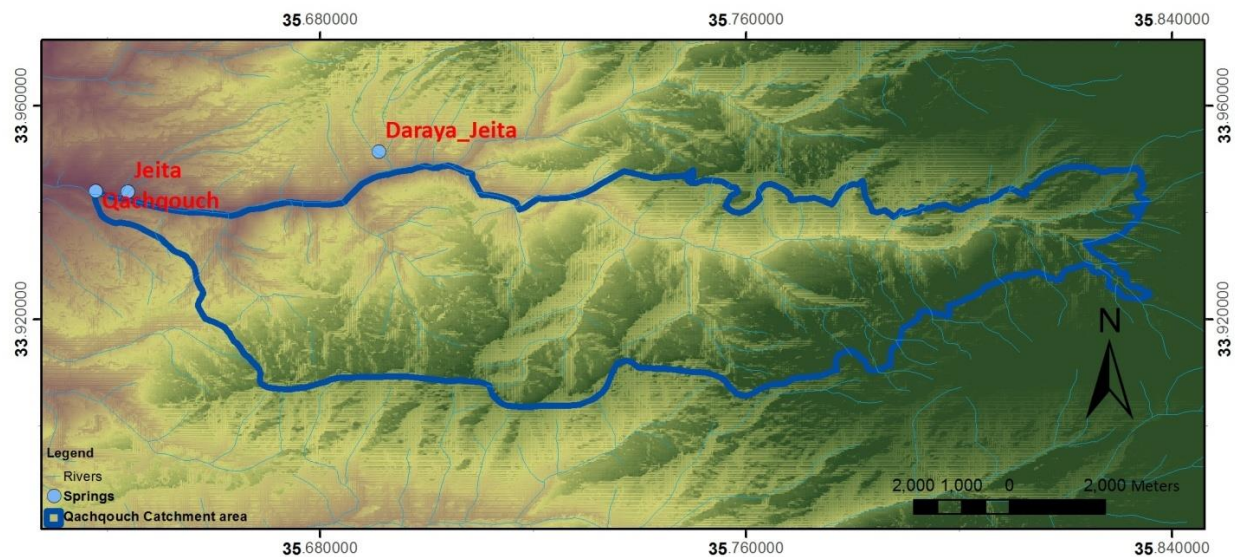


Figure 4.1. The catchment area of the investigated Spring (Qachqouch). Nahr el Kalb River acting as a boundary condition in the northern part of the catchment.

4.2 Methodology

The aim of this study is (1) to show the map of the spatial distribution of the recharge in mm, i.e., the estimation of the percentage of water from the total precipitation that reaches the water table of the investigated Qachqouch karst aquifer in Lebanon using the APLIS method; (2) The average of recharge from APLIS method is compared with the estimated recharge using other methods for the same aquifer and assessed in light of the uncertainties in the base maps used in the evaluation of recharge.

The assessment of the recharge of the Qachqouch spring catchment using the APLIS method requires a robust investigation of the factors affecting recharge. Therefore, data related to the inherent geological and hydrogeological characteristics of the catchment, mainly to surface features and catchment parameters, including climatic data, land use land cover, soil, topography, lithology, karst features were collected, processed, converted to Raster and overlain to produce the final recharge map. This section provides an overview of the major investigated layers used in the APLIS Method (Table 4.1)

Table 4.1

Table 4.1. Raw data and Layers (type and reference) required for the APLIS method.

Shapefile/layer	Reference	Type of data	Resolution
Precipitation	Based on measurement (2014-2020) Assessment of historical data to determine the precipitation gradient	Time series	30-min; average yearly precipitation
*Topography	Digital Elevation Model (DEM) for Lebanon	DEM Raster	30 m resolution
Soil (texture and thickness)	Soil map for Lebanon (1955)	Polygon	1:50000
Geology	Dubertret (1955)- Hahne et al., 2011 Field mapping	Polygon	1:20000
Dolines (Point source)	Mapped on satellite imagery and validated in the field	Polygon	1:25000
*Base map resolution for the raster layers			

The shapefiles were processed with ARC GIS (version 10.3), using various tools, like the **conversion tools** to transform shapefiles into a raster layer for mathematical calculations, **spatial analyst tool, the Math tool** for the calculation of raster layers according to the weight attributed to each attribute. Resultant rasters were reclassified into classes as required by the respective method. This section briefly summarizes the type of data, their acquisition, and their processing into adequate shapefiles used in the generation of the recharge map. The World Geographic System (WGS 1984) map projection was adopted for the entire database. The different layers were first reproduced as shapefiles (vector) and were then converted into a 30 m cell unit grid that represents the cell size of the DEM as follows (Figure 4.2).

- Altitude: The DEM was clipped and reclassified into ten categories based on APLIS weight classification using the “reclassify” tool in the ArcToolbox-Spatial Analyst Tool-Reclass. As the

altitude increases, recharge increases. Thus, a high weight was given for high altitudes in the new classification.

- Slope: A slope in percentage map was generated from the clipped DEM using the “Slope” tool in ArcToolbox-Spatial Analyst Tool-Surface. A new classification was done into ten categories showing high infiltration and recharge in areas of low slope. This relation relies on the fact of fast surface runoff of rainfall in areas of high slope percentage and slope degree.
- Lithology: a geological map was converted to raster and was reclassified as follows: Formations of Jurassic and Cretaceous are represented by J4, J5, J6, and J7 for Jurassic layers and C1, C2a, C2b, C3, and C4 for the Cretaceous ones. Higher weights were given to karst carbonates J6 and J4 (limestone and dolostones), respectively, while the minimum weight was attributed to volcanic rocks and marls (Table 4.2).
- Infiltration: This layer includes dolines, faults, fractures, vegetation, and urbanization. Dolines were given a weight of 10 while areas with high urbanization or vegetation were classified with a weight less than 5.

Altitude (A)			
description		weight	
<300		1	
300-600		2	
600-900		3	
900-1200		4	
1200-1500		5	
1500-1800		6	
1800-2100		7	
2100-2400		8	
2400-2700		9	
>2700		10	

SloPe (P)		
description		weight
>100		1
100-65		2
65-45		3
45-30		4
30-20		5
20-15		6
15-10		7
10-5		8
5-3		9
<3		10

Lithology (L)			
Description	Age	symbol	weight
Volcanics	Upper Jurassic	J5	2
Marly Limestone	Upper Aptian	C3	3
Sandy Limestone	Aptian	C2a	5
Limestone	Upper Jurassic	J7	5
Sandstone	Lower Cretaceous	C1	6
Limestone	Aptian	C2b	7
Dolomite-limestone	Cenomanian	C4	10
Limestone	Upper Jurassic	J6	10
Dolomite-limestone	Middle Jurassic	J4	10

Infiltration (I)	
description	weight
high impermeability (with or no vegetation)	3
low urbanisation (villages)+vegetation+karstificati	5
High vegetation + karstification	7
low vegetation+karstification (flanks bare rocks)	8
karstification (dolines, faults)	10

Soil (S)	
description	weight
grey soil	3
black soils (volcanics)	2
yellow-grey soils	3
sandy soils	9
mixed soils (sandy-marly)	4
mixed soils	3
terra rossa (calcareous soils)	10
landslides and mass wasting	3

Correction Factor (Fh)	
description	weight
J5/J6/J7/volcanics/C1/C3	0.1
J4/C2a/C2b/C4	1

classification of rate of recharge	
rate of recharge (%)	class
0 - 20	very low
20 - 40	low
40 - 60	moderate
60 - 80	high
80 - 100	very high

Figure 4.2 Weights assigned to attributes for APLIS layers according to available coverage information and literature.

Table 4.2. Classification of the geological formations according to their permeability.

Type of lithology	Nomenclature	Age	Value_APLIS (L)
Limestones, highly karstified	J4/j6	Jurassic	10
Fissured fractured limestones	C2b	Cretaceous	7
	C2a/J7	Cretaceous, Jurassic	5

Type of lithology	Nomenclature	Age	Value_APLIS (L)
Fractured sandstones	C1	Cretaceous	5
Marly limestones	C3	Cretaceous	3
Basalts	J5	Jurassic	2

- Soil: The vector layer was converted to a raster and then it has been reclassified into soil types in Andreo et al. (2008) and Farfan et al. (2010). While calcareous soil was attributed a weight of 10 and sandy soil the weight of 9, volcanic black and gray soils were classified as low magnitudes of 2 and 3 respectively.

The overlay (addition) of the weighted attributes yielded an output layer of the distribution of recharge all over the catchment, in other words, the output map represents the percentage of rainfall that may reach the water table as recharge from the total precipitation (R) in each cell of 30×30 m dimensions. Details about raw data, classifications, and reclassification of each APLIS layer are presented in Table 4.4.

- Precipitation

The spatial distribution of recharge in mm is a product of the recharge (in percentage) and total precipitation distribution over the catchment area in mm. The precipitation/ altitude gradient reaches, on average, +20 mm per increments of 100 m in altitude (based on the comparison of rainfall amounts between 14 m and 805 m above sea level). Additionally, data from the climatic station at 950 m.a.s.l. from 2014 till 2020 shows an annual average of 1200 mm. A raster layer for precipitation distribution was generated from the clipped DEM based on the variation of altitude using Equation 4.1. The raster precipitation distribution is calculated based on the collected high-resolution data at 950 m asl (Table 4.).

Table 4.3. Total precipitation for different types of years (dry, intermediate, wet) used in the interpolation of P over the catchment.

Type of year	Total Precipitation (mm)	
	Value at 60 m asl	Value at 950 m asl
Dry year	743mm	921 mm (2015-16)
Average to dry year	856 mm	1034 mm (2016-17)
Average year	911 mm	1089 mm (2017-18)
Wet year	1312	1490 mm (2018-19)

$$P(Z) = P(950) - ((950 - Z) * \frac{20}{100}) \quad \text{Equation 4.1}$$

Where P (Z) is the annual precipitation at an altitude Z on the catchment in [m]; P(950) is the reference precipitation collected on the catchment. 20 mm is the precipitation gradient per 100 m elevation.

Table 4.4. Raw data for the Qachqouch case study processed according to the classification criteria of the APLIS method.

Item	Name/ description	Criteria	Raw data	Processed data and raster	Initial classification	Reclassification	Data gaps
A	Altitude	Altitude in meters: 45<altitude<1619	-DEM for altitude (30-m) for Lebanon WGS 1984 Geographic (raster)	-“Extract by mask” tool -“Reclassify” tool	<300 301-600 601-900 901-1200 1201-1500 1501-1800	1 2 3 4 5 6	None
P	Slope	Slope in percentage	-DEM for altitude (30-m) for Lebanon WGS 1984 Geographic (raster)	-“Slope” tool -“Reclassify” tool	>100 100-65 65-45 45-30 30-20 20-15 15-10 10-5 5-3 <3	1 2 3 4 5 6 7 8 9 10	None
L	Lithology	Geological maps of Lebanon (1:50000)	Geology map shapefile (vector)	-“add field” to contribute table -reclassify the new field -“polygon to raster” tool	Volcanics (J5) Marls C2a/J7 C1 C2b J4/J6	2 3 5 5 7 10	Detailed mapping of dolostone tongues within the J4
I	Infiltration	Digitized map	Google Earth imagery (vector)	-digitizing by “editor” on imagery base map -“polygon to raster” tool	-high impermeability (with or no vegetation) -Urban (villages)+ vegetation+ karst -High vegetation + karst -Low vegetation+karstification (flanks bare rocks) -karst (dolines, faults)	3 5 7 8 10	-Higher-resolution Remote sensing and field validation for doline delineation -Evaluation of fault permeability
S	Soil	Soil of Lebanon	Types of soil shapefile (vector)	-“add field” to contribute table -reclassify the new field -“polygon to raster” tool	-black soils -gray/yellow soil/ landslides -mixed soil -sandy soil -calcareous soils	2 3 4 9 10	Soil thicknesses
Fh	Correction factor	Reference: Hartmann et al. 2014	Rate of recharge map from raster calculator	-“reclassify”	C3/J5/J7/C1 (volcanic/sandstone) C2a/C2b/C4/J4/J6 (limestones)	0.1 1	Sensitivity analysis of model to correction factor
Pr	Precipitation	Variation of precipitation (5.5% with 100m elevation) Reference: Doummar 2018	-DEM for altitude (30-m) for Lebanon WGS 1984 Geographic (raster)	-“extract by mask” tool -“reclassify” tool	Data years (2014-2020) from 2 stations (at 950 m and 1750 m) in Mount Lebanon from 2016 to 2019 and historical data (2000-2010) for Beirut area (14m above sea level).	isohytes	Stations should cover the different climatic areas in Lebanon + more years are required for average calculations

The Precipitation distribution for an average year is shown in Figure 4.3.

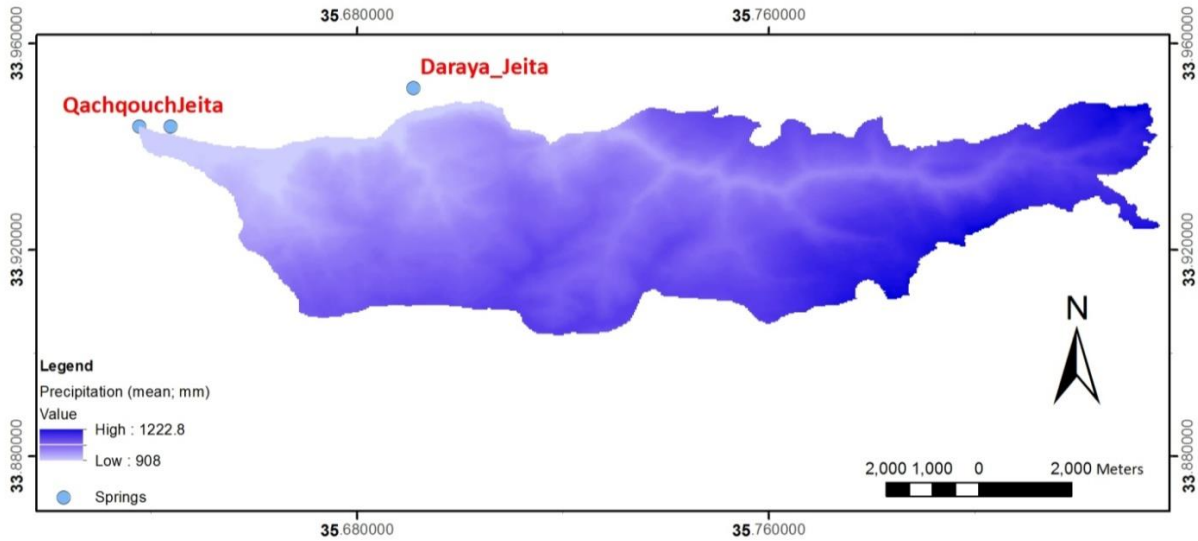


Figure 4.3. Precipitation distribution for an average year.

4.3 Results

4.3.1 Individual layer Output

Figures 4.4 to 4.8 were overlain using Raster Math with the respective weights for each factor and then corrected with the correction factor layer (Figure 4.9) to compute the total recharge percent per increments of 5% for the total area (Figure 4.10).

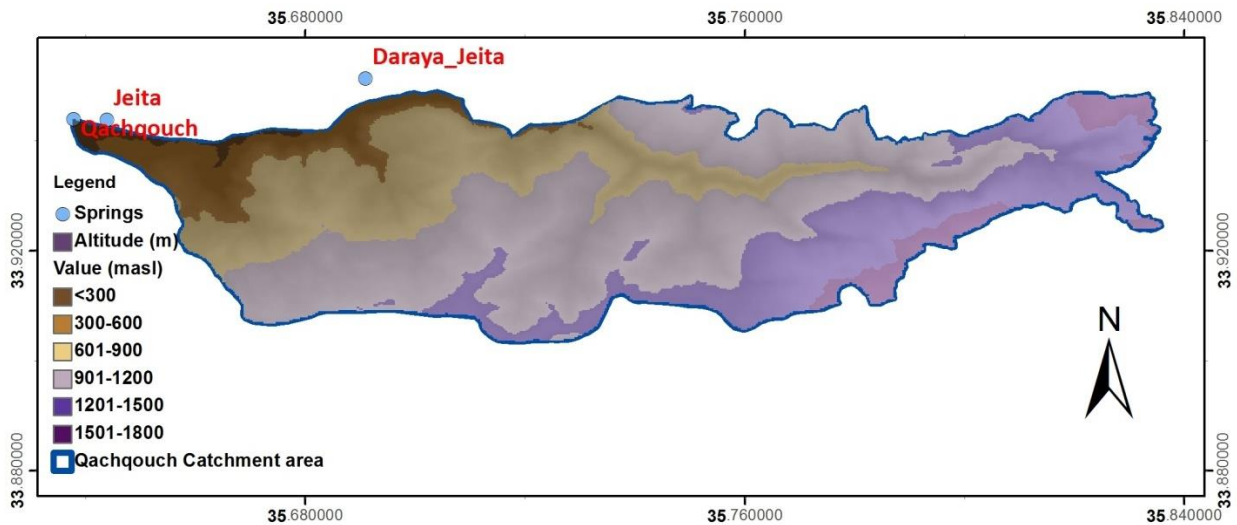


Figure 4.4. Layer A (Altitude).

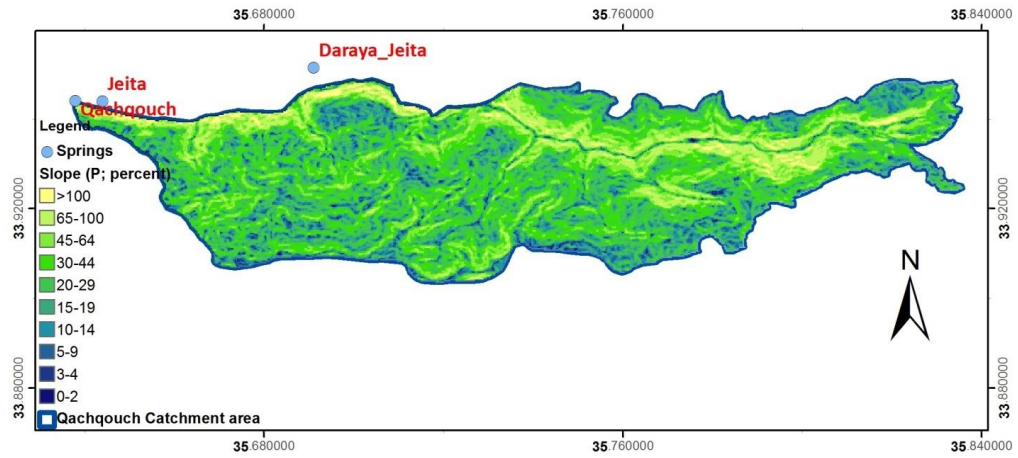


Figure 4.5. Layer P (Slope).

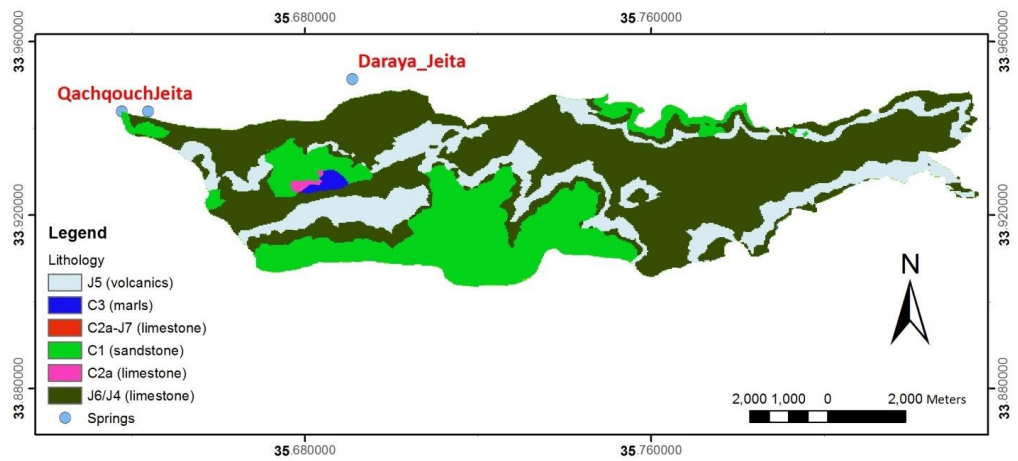


Figure 4.6. Layer L (Lithology).

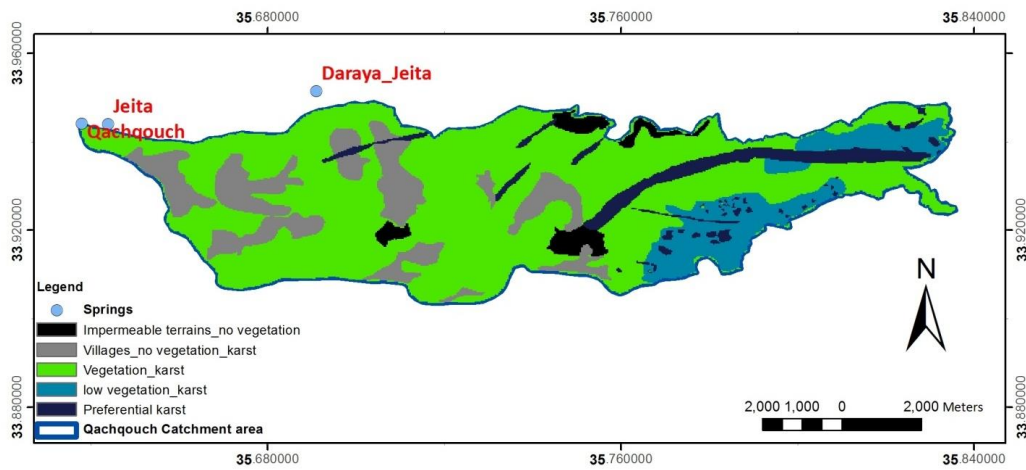


Figure 4.7. Layer Infiltration (I).

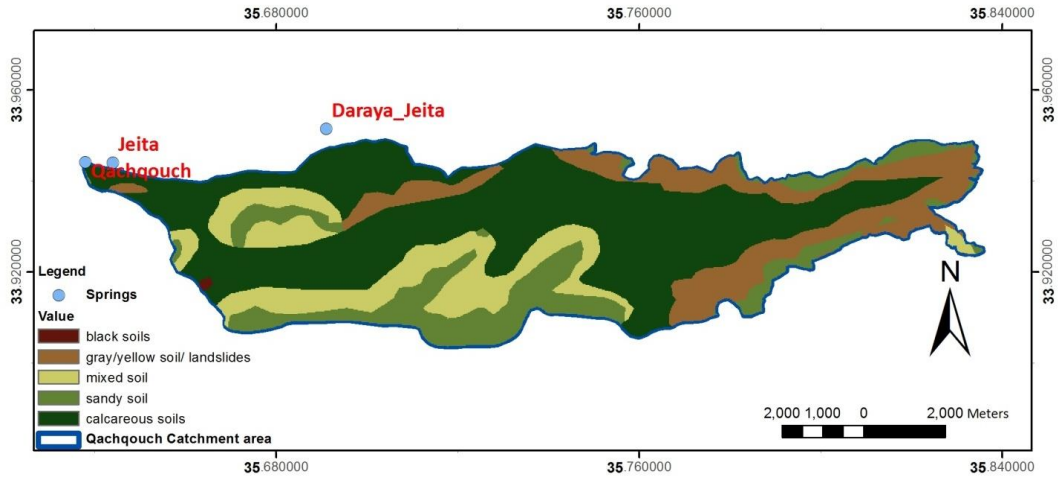


Figure 4.8. Layer S (Soil).

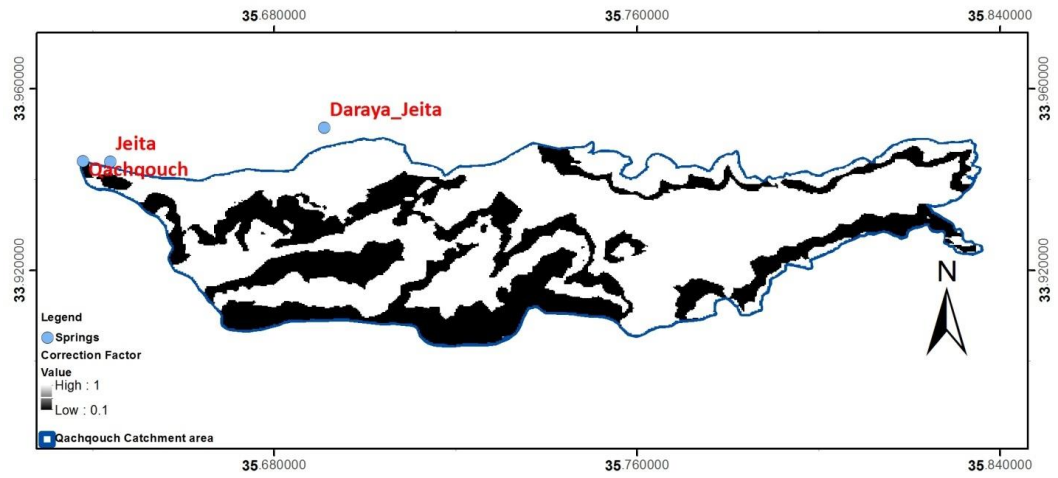


Figure 4.9. Correction Factor layer.

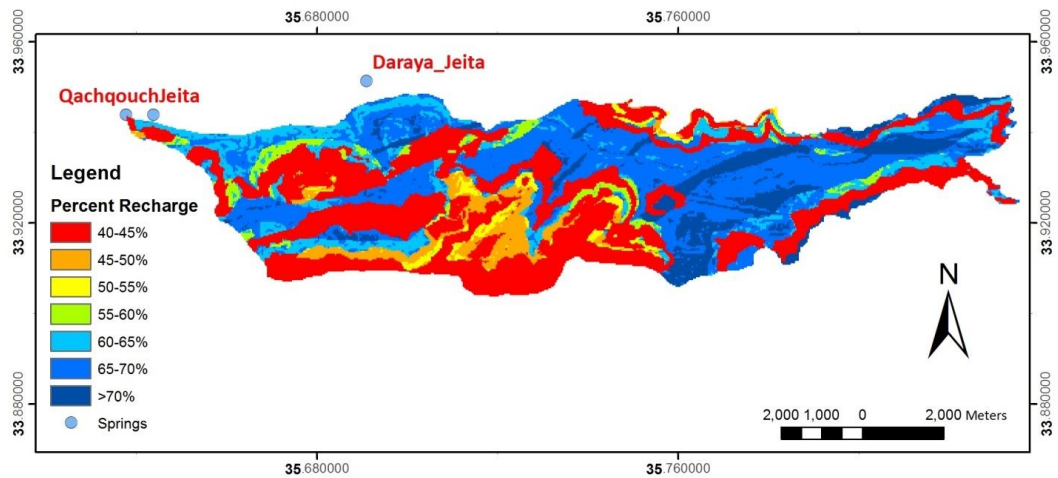


Figure 4.10. Percent Infiltration (in 5% increment) using the APLIS method.

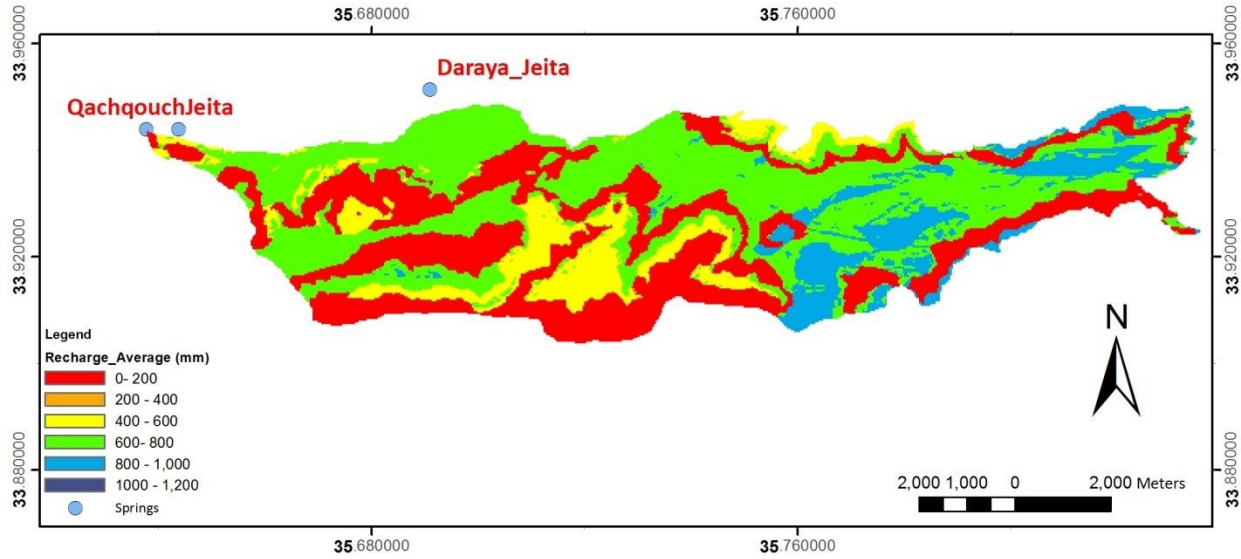
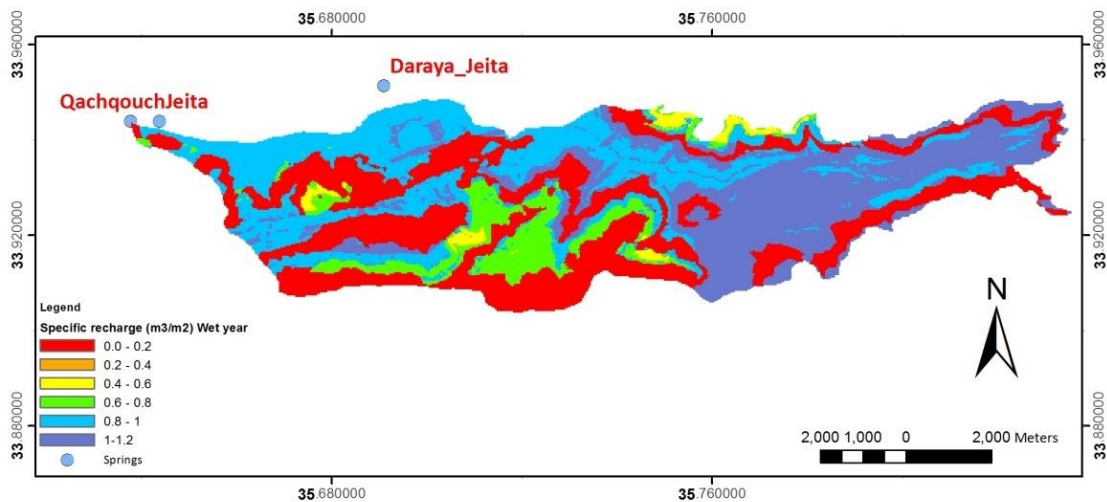


Figure 4.11. Final recharge map in mm (Using APLIS) for an intermediate year.

4.3.2 Total Recharge and Areal Distribution

The variation of the areal distribution of the recharge percentages is shown in Figure 4.12. The variation of the aerial distribution of the recharge percentages is shown in Table 4.5. for varying hydrological regimes. The total recharge calculated over the catchment area amounts to an average of 25.6 Mm^3 ($\pm 5 \text{ Mm}^3$) per year in an intermediate hydrogeological year (mean total precipitation of 1000 mm). According to APLIS, the values for recharge are 22.1 and 27.5 Mm^3 for a dry and wet year respectively. The areal distribution of precipitation is shown in Table 4.5. Figure 4.13 shows the variation of the areal distribution of the ranges of specific recharge between a wet, intermediate, and dry year.



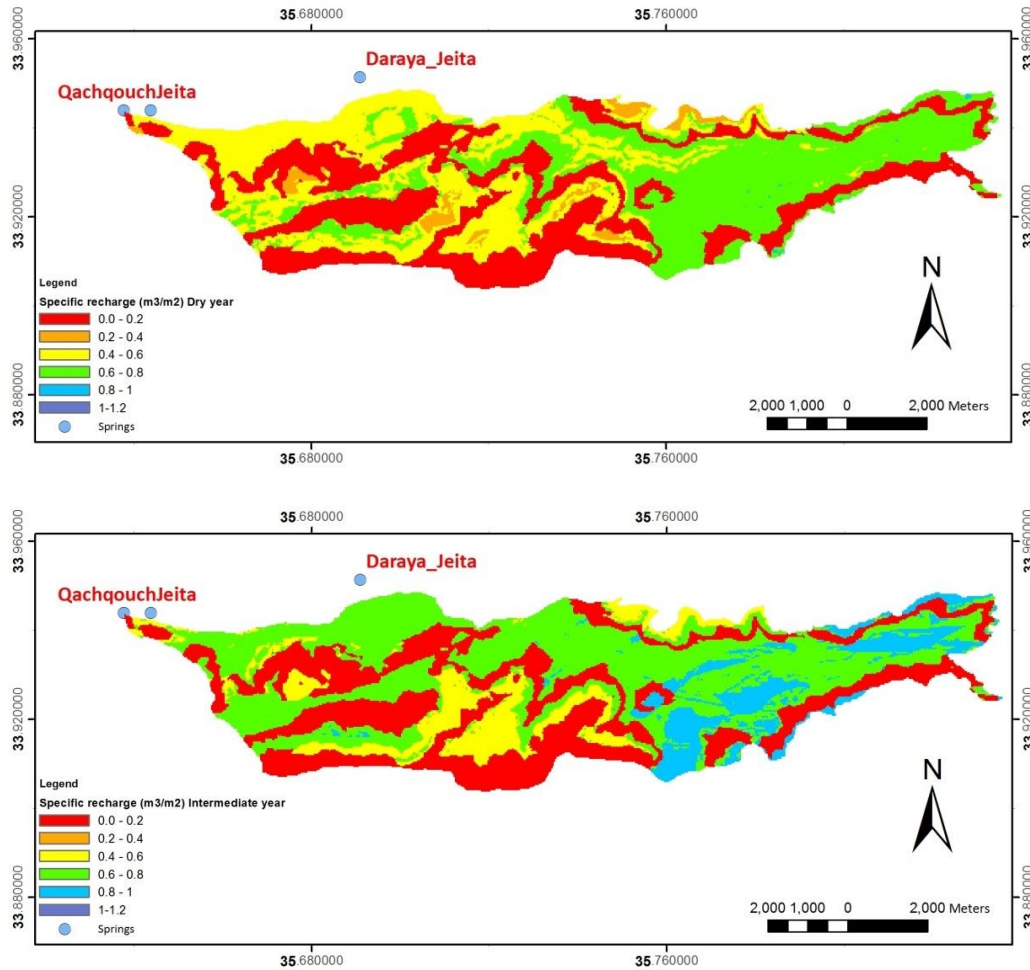


Figure 4.12. Specific recharge (m^3/m^2) for years of wet, dry, and intermediate Precipitation.

Table 4.5. Recharge classes, areas, and total average recharge values in m^3 per class area and as a percentage of the total area (A_t) as computed with APLIS.

Class (mm)	Wet year			Dry year			Intermediate year		
	Area (km ²)	Volume (Mm ³)	% of A_t	Area (km ²)	Volume (Mm ³)	% of A_t	Area (km ²)	Volume (Mm ³)	% of A_t
0-200	17.64	1.8	34%	17.64	1.8	34%	17.64	1.8	34%
200-400	0.97	0.3	2%	1.41	0.4	3%	0.01	0.0	0%
400-600	4.40	2.2	8%	15.17	7.6	29%	6.12	3.1	12%
600-800	14.20	9.9	27%	17.55	12.3	34%	22.44	15.7	43%
800-1000	14.24	12.8	27%	0.05	0	0%	5.62	5.1	11%
1000-1200	0.38	0.4	1%	0.00	0	0%	0.00	0.0	0%
Total (Mm³)		27.5	±5 Mm³		22.1	±5 Mm³		25.6	±5 Mm³

* $A_t=51 \text{ km}^2$

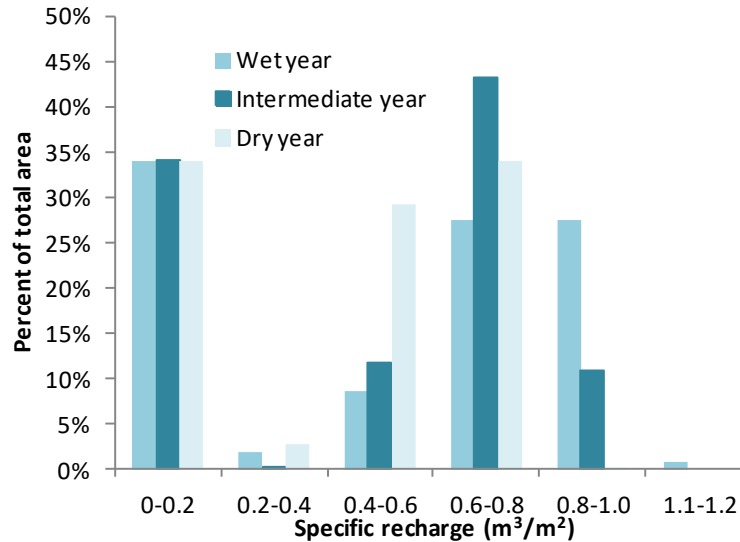


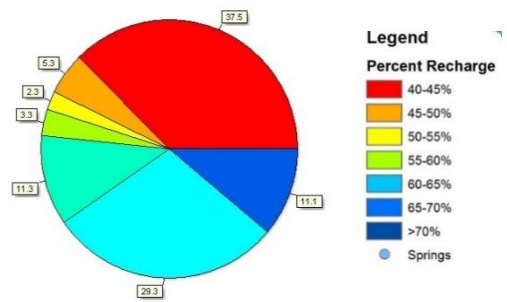
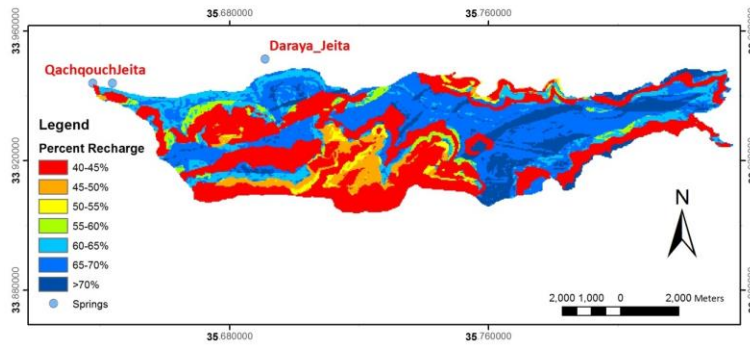
Figure 4.13. Specific recharge distribution in percent and variation according to the hydrological regime between dry, intermediate, and wet years.

4.4 Discussion and Model Sensitivity

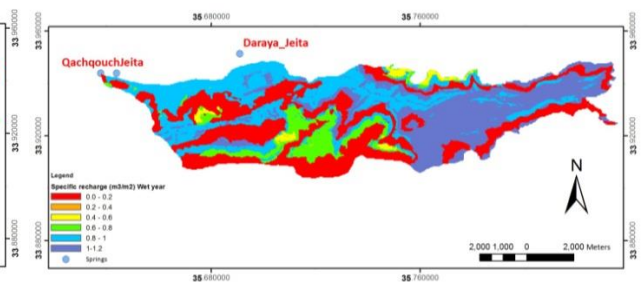
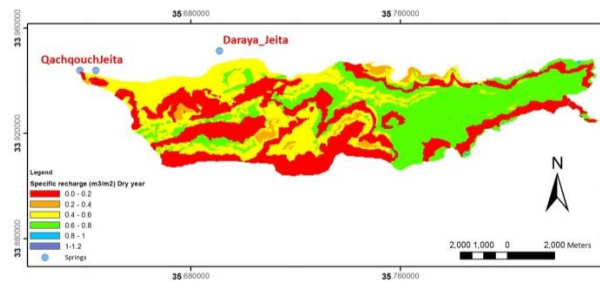
- The amount of specific recharge per area was successfully estimated using APLIS for the catchment area of Qachqouch and revealed that substantial recharge (60% and above of precipitation) occurs on a large area over the Spring catchment, indicative of its karstic nature and predominance of point source infiltration.
- The total volume observed at the spring ranges between 30-50 Mm³ depending on the amount of precipitation. Spring volumes may be overestimated during high flow periods because of the difficulty of measurements. On the other hand, the amounts estimated using APLIS may vary according to the rain intensity, overland flow from layers outside the catchment, and saturation in the subsurface. However, the amount of recharge estimated using APLIS falls well within the ranges of spring discharge.
- A sensitivity analysis will allow a better understanding of the effect of varying APLIS parameters on the resulting recharge map.

The final recharge map is highly dependent on the resolution of the different layers that play a role in recharge according to the APLIS method. The results could be further improved if the following is further investigated:

- The resolution of the Digital Elevation model yielding the layers **Altitude** and **Slope** is found to be suitable for the scale of recharge investigation;
- **Lithology**: The lithology classification could be further detailed to include the dolostone tongues in the upper part of the catchment as well as the one present along leaky faults. A potential overland flow over formations located outside the catchment area could also be included in the area of investigation as contributing to the recharge over the Jurassic layers;

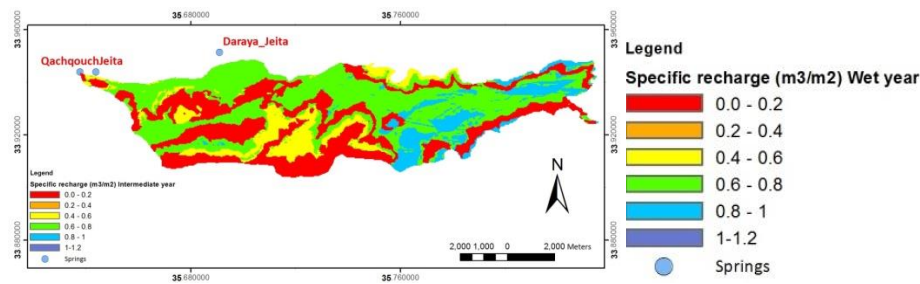


Percent Infiltration (in 5% increment) using the APLIS method



Specific recharge (Dry year)

Specific recharge (wet year)



Specific recharge (Intermediate year)

- Detailed mapping of the point source features and land use land cover on a higher resolution satellite imagery should help to decrease the uncertainty in the layer **Infiltration**. Furthermore, tracer experiments planned in selected dolines will allow the delineation of fast infiltration points and hydrogeological connections, and thus, APLIS results can be improved.
- The distribution of **Precipitation** over the catchment can be further refined with a better assessment of the precipitation gradient variation with altitude.

A sensitivity analysis on the impact of the **Correction Factor** over the resultant map.

4.5 References

- Andreo, B., Vías, J., Durán, J.J., Jiménez, P., López-Geta, J.A., Carrasco, F. Methodology for groundwater recharge assessment in carbonate aquifers: application to pilot sites in southern Spain. *Hydrogeology Journal*. 16 (5): 911–926, 2008.
- Bakalowicz, M., Karst, and Karst Groundwater Resources in the Mediterranean. *Environ Earth Sci Environmental Earth Sciences* 74, no 1: 5-14, 2015.
- Doummar, J. and Aoun, M. Occurrence of selected domestic and hospital emerging micropollutants on a rural surface water basin linked to a groundwater karst catchment, *Environmental Earth Sciences*, 77(9), 351, doi: 10.1007/s12665-018-7536-x, 2018b.
- Dubertret, L., Carte Geologique detaillee du Liban. Beyrouth : Ministere des travaux Publics. 1955
- Dubois E., Doummar J., Pistre S., Larocque M. Calibration of a semi-distributed lumped model of a karst system using time series data analysis: the example of the Qachqouch karst spring. *Hydrol. Earth Syst. Sci.*, 24, 4275–4290, doi.org/10.5194/hess-24-4275-2020, 2020.
- Dubois, E: Analysis of high-resolution spring hydrographs and climatic data: application on the Qachqouch spring (Lebanon), Master thesis, American University of Beirut, Department of Geology, Beirut, Lebanon. 2017. [online] Available from: https://www.researchgate.net/profile/Emmanuel_Dubois5/publication/320237930_Analysis_of_high_resolution_spring_hydrographs_and_climatic_data_application_on_the_Qachqouch_spring_Lebanon/links/59d69a76a6fdcc52aca7d05c/Analysis-of-high-resolution-spring-hydrographs-and-climatic-data-application-on-the-Qachqouch-spring-Lebanon.pdf, 2017.
- Farfán, H., Corvea, J., de Bustamante, I. Sensitivity Analysis of APLIS Method to Compute Spatial Variability of Karst Aquifers Recharge at the National Park of Viñales (Cuba). In: Andreo B., Carrasco F., Durán J., LaMoreaux J. (eds) *Advances in Research in Karst Media*. Environmental Earth Sciences. Springer, Berlin, Heidelberg., 2010.
- Hahne, K., Abi Rizk, J., and Margane, A. Geological Map of the Jeita Groundwater Contribution Zone. - German-Lebanese Technical Cooperation Project Protection of Jeita Spring, Technical Report. Raifoun. 2011
- Hartmann, A., Mudarra, M., Andreo, B., Marín, A., Wagener, T., Lange, J. Modeling spatiotemporal impacts of hydroclimatic extremes on groundwater recharge at a Mediterranean karst aquifer. *Water Resour. Res.* 50 (8), 6507–6521, 2014.
- Nader, F. H, and Swennen, R. The hydrocarbon potential of Lebanon: New insights from regional correlations and studies of Jurassic Dolomitization. *JPG Journal of Petroleum Geology* 27, no 3: 253-75, 2004.

5 Ubrique test site (case study Spain)

5.1 General description of the test sites

Both Eastern Ronda Mountains and Sierra de Ubrique aquifer systems are quite representative of mountainous carbonate aquifers in the Spanish Mediterranean area, showing highly variable recharge and limited groundwater resources. From a geological standpoint, the study area is located in the western sector of Betic Cordillera. A complete geological description has been previously included in D2.1 Water balance.

The **Merinos-Colorado-Carrasco** test site presents outcrops of Flysch sandstones and clays (Cretaceous-lower Miocene) represented in the eastern sector (Fig. 5.1), overthrusting previously described geological formations. Discordant above all these upper Miocene calcareous sandstones are found, belonging to the sedimentary infilling of the Ronda basin, in the western part.

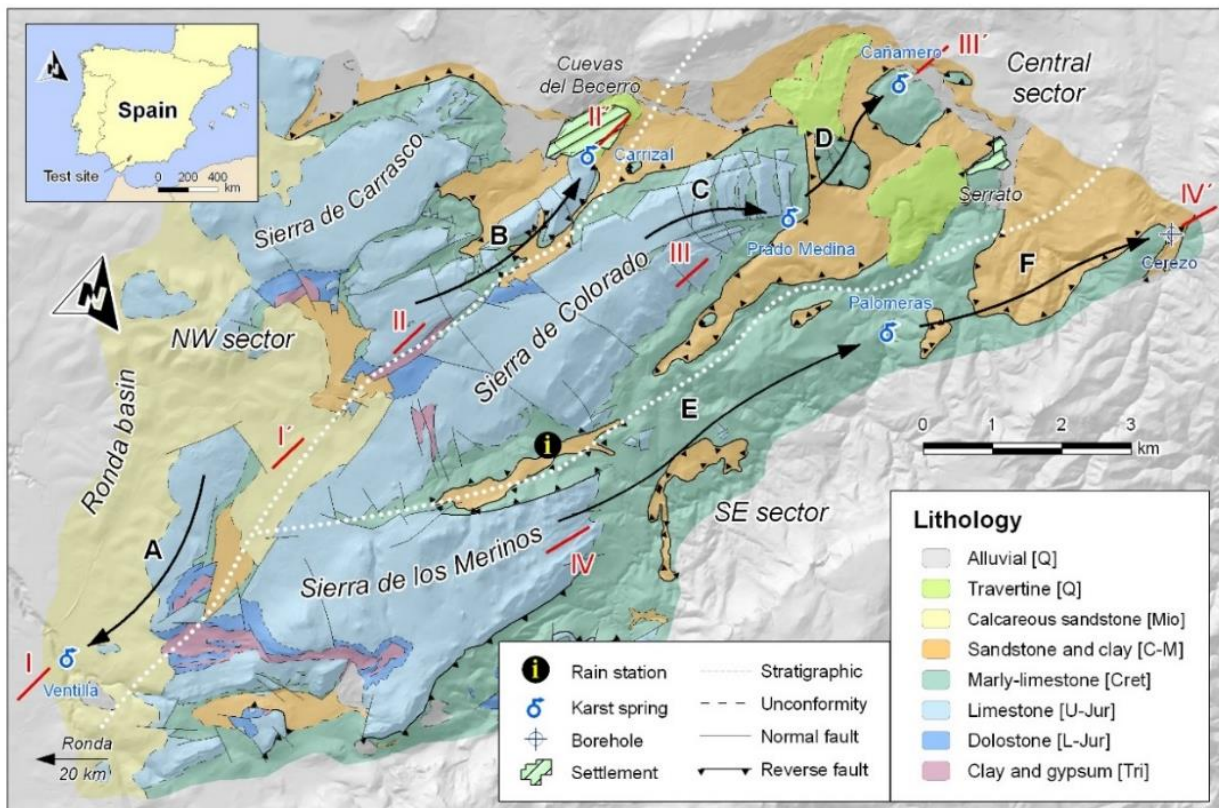


Figure 5.1. Hydrogeological setting of Merinos, Colorado and Carrasco aquifer systems (Barberá et al., 2012).

From a hydrogeological outlook, Jurassic limestones cover a large area in the test site and these (aquifer) lithologies are represented on surface, as karst exposures, or in depth, as buried aquifer segments. Dolomitic rocks, which comprise the lower levels of the Jurassic aquifers, can reach higher positions in the lithological sequence, and even appear on surface. Gypsum bearing formations (Triassic clays with gypsum), whose thickness is still imprecise, constitute the lower limit of the main aquifers and can uplift through faults.

Sierra de Ubrique test site is placed within Sierra de Grazalema Natural Park, in the eastern part of the Cádiz province and 35 km of distance from Merinos-Colorado-Carrasco area. Aquifer formations in this area are also developed in Jurassic dolostones and limestones, resulting in highly fractured and

karstified systems (Fig. 5.2) (Martín-Rodríguez et al., 2016). In the same way that happens in Eastern Ronda Mountains, clays and sandstones overthrust the previous geological formations in exception of some zones where Flysch materials structurally imbricate between Mesozoic rocks in the “Corredor del Boyar” (Martín-Algarra, 1987). This corridor provokes the individualization of two hydrogeological systems: one in the north (subbetic sector) and one in the south (penibetic sector), in which the Sierra de Ubrique is included (Fig. 5.2) (Martín-Rodríguez et al., 2016).

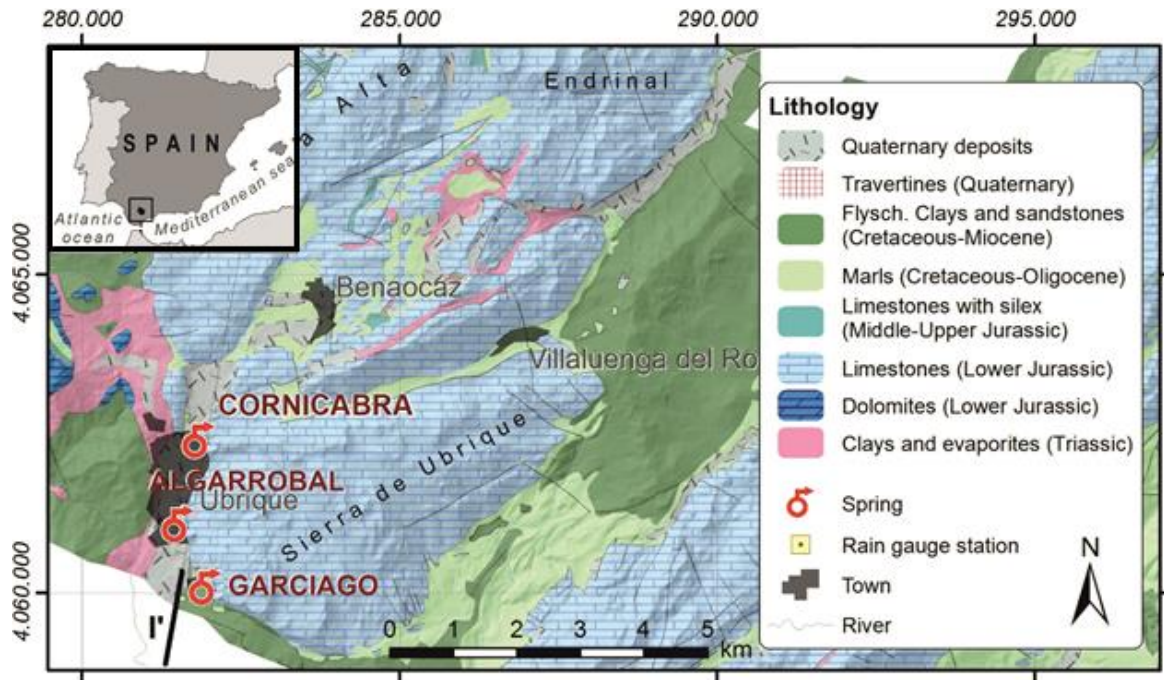


Figure 5.2. Hydrogeological setting of the Sierra de Ubrique aquifer system (modified from Sánchez et al., 2017).

5.2 Technical information about input layers

The main goal of this report is to estimate the effective rain rate at the study area and to graphically represent the spatial distribution of the recharge. The application of the APLIS method at the Eastern Ronda Mountains test site have been previously described (Barberá, 2014), however, it supposes the first assessment of the spatial recharge distribution at the Ubrique test site.

The following tables (Tab. 5.1 and 5.2) summarize the characteristics of each input layer at both test sites:

Table 5.1. Input layers for GIS processing at Merinos-Colorado-Carrasco test site (Barberá et al., 2014).

Layer	Retrieved from	Resolution	Comments
Altitude	National Geographic Institute	5x5 m	Developed in 2008
sloPe	Elevation Digital Model		
Lithology	Spanish Geological Survey	5x5 m	Continuous digital geological map 1: 50.000
Infiltration	Field observations	5x5 m	Map developed through fieldwork and geological information
Soil	Soil Map of Andalusia 1: 400.000	5x5 m	Developed in 2005

At **Merinos-Colorado-Carrasco** test site recharge takes place by the infiltration of rainwater through limestone and dolostone outcrops. The soil is non-existent in many places in this area due to the lithology (limestones, dolomites, marls and marly-limestones) and the slope, so that agricultural land uses are scarce.

Surface karstification is controlled by the type of lithology, the geological structure, and the rainfall regime of the region. Among the carbonate materials, the development of karstification is higher in the limestones. In the upper parts of the main massifs, the “boxed” anticline structure, with the sub-horizontal strata in the hinge, promote the karstification processes of the Jurassic limestones. The low inclination of the layers ($<20^\circ$) allows the formation of endorheic areas and hinders the generation of surface runoff (Barberá, 2014).

Table 5.2. Input layers for GIS processing at the Ubrique test site.

Layer	Retrieved from	Resolution	Comments
Altitude	National Geographic Institute	5x5 m	Developed in 2018
sloPe	Elevation Digital Model		
Lithology	Spanish Geological Survey	5x5 m	Continuous digital geological map 1: 50.000
Infiltration	Field observations	5x5 m	Map developed through fieldwork and geological information
Soil	Soil Map of Andalusia 1: 400.000	5x5 m	Developed in 2005

In the same way that was realized in the previous case, the final five APLIS layers are obtained for the Ubrique test site after computing and reclassifying the input layers. Figure 5.3 shows the detail and spatial distribution of each GIS layer for the Ubrique test site.

In this case, recharge takes place mainly by the infiltration of rainwater through limestone outcrops and an allogenic recharge which enters the system through the Villaluenga del Rosario shaft. The most parts of the recharge area range between 600 and 1200 m.a.s.l. and present abundant surfaces with a slope below 30%, which cause very low runoff generation. Lithology favors the development of karstification, and thus, infiltration landforms such as karren fields and dolines can be found over the carbonate outcrops especially in the top areas. Some of the dolines and swallow holes that exist in this area are highly developed and numerous speleological expeditions have been documented. The development of thin soils also promotes diffuse infiltration and no agricultural activities are found, so that the main land use is livestock (goat and sheep).

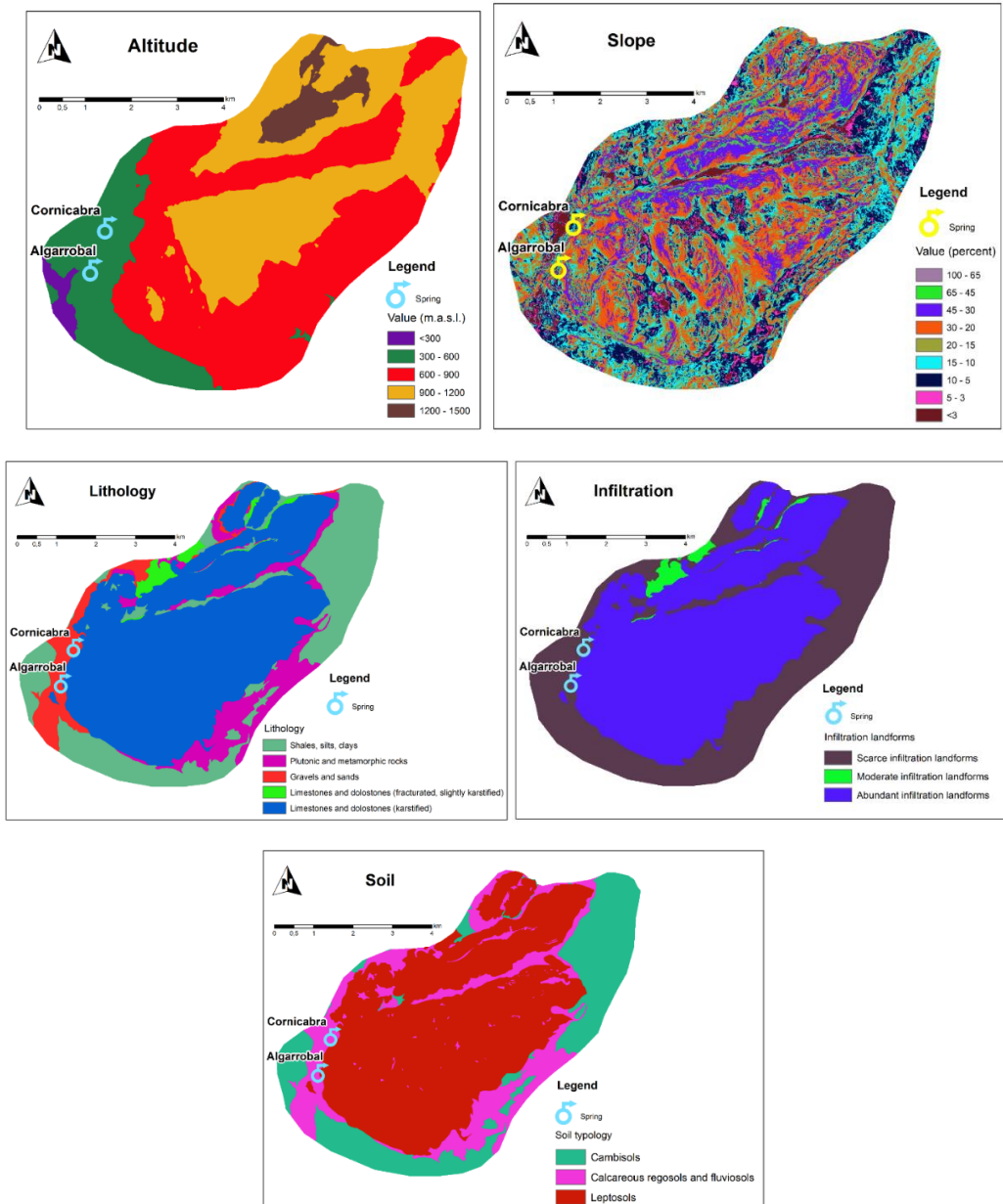


Figure 5.3. Input layers for the application of the APLIS method at the Ubrique test site.

5.3 Precipitation

The analysis of the spatial distribution of rainfall at **Merinos-Colorado-Carrasco** test site has been carried out from the isohyets maps (Fig 5.4) corresponding to a wet year (2009/10), a dry year (1998/99) and the average year cases of the period 1964/65-2009/10 (Barberá, 2014). The layout of the isohyets is relatively similar in the dry and middle years, however, the wet year disposes a slightly different shape, so that the northern and southern parts (Sierra de Carrasco and Sierra de los Merinos) of the study area receive more precipitation than the central part (Sierra de Colorado). The mean annual precipitation for the wet year is 1,194 mm, 733 mm for the average year and 327 mm in the dry one.

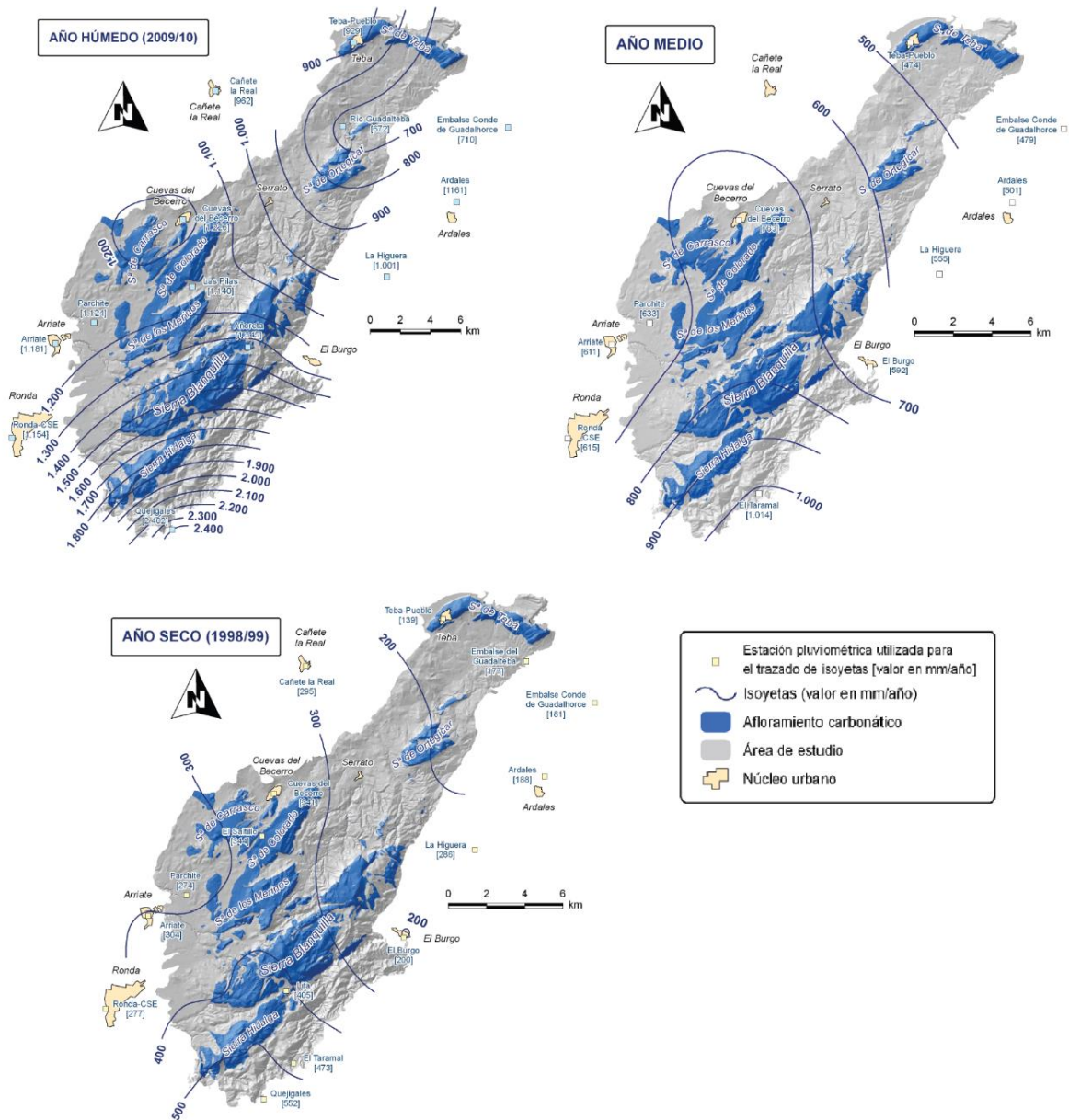


Figure 5.4. Spatial distribution of rainfall at the Eastern Ronda Mountains test site (Barberá, 2014).

The spatial distribution of rainfall at the **Ubrique** test site has also been obtained through a GIS interpolation of weather station data and was then transformed into a contour map. Different maps (Fig 5.5) were realized corresponding to a wet year (2009/10), a dry year (2004/05) and the average year cases of the period 84/85-17/18 (Thesis in preparation).

The final disposition of the isohyets is relatively similar in the three cases, showing increasing precipitation to the NE (Fig 5.5), however, the precipitation gradient substantially changes from one scenario to another, increasing for wet and average years. The mean annual precipitation for the wet year is 2,384 mm, 1,297 mm for the average year and 531 mm for the dry one.

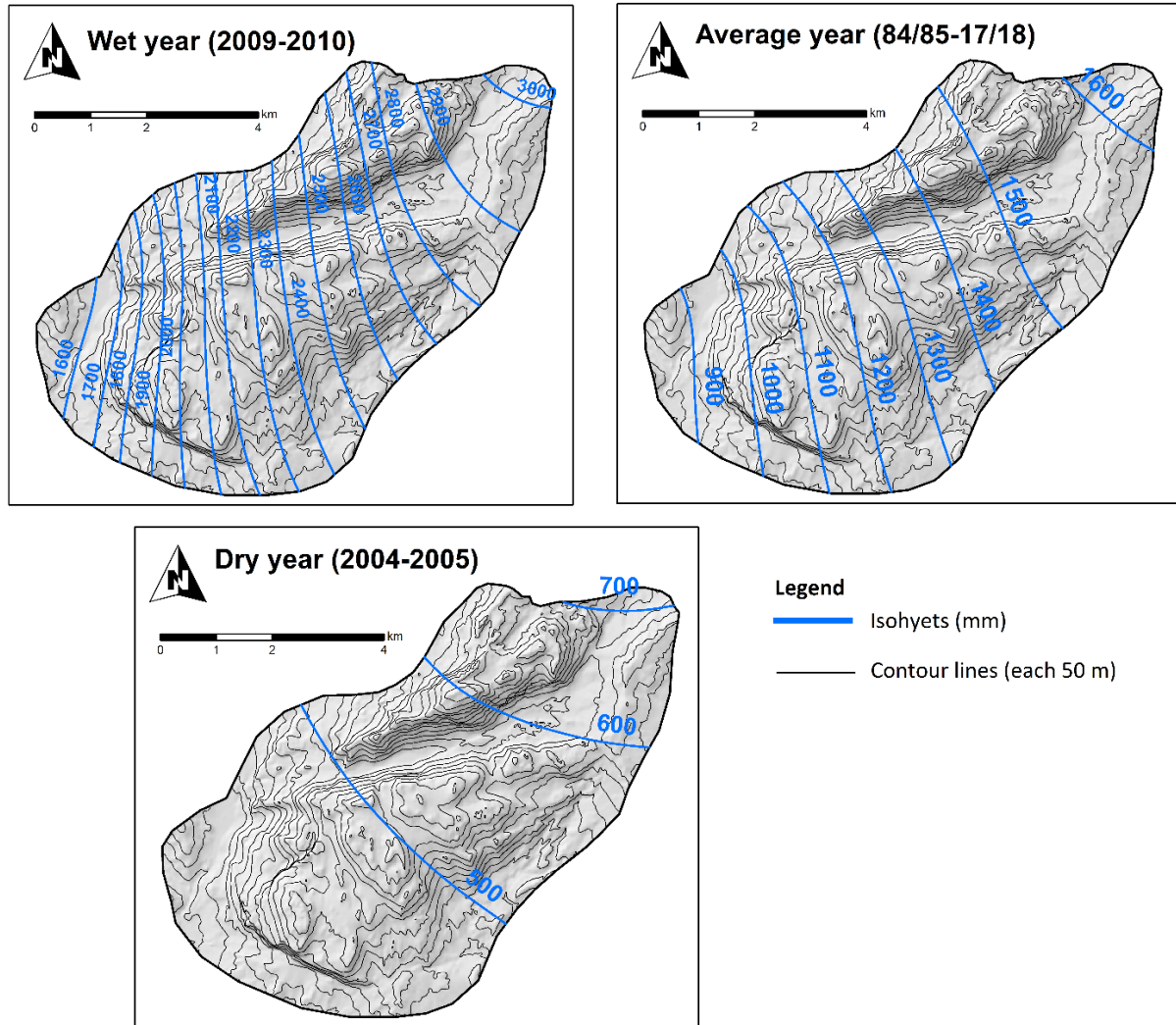


Figure 5.5. Spatial distribution of rainfall at the Ubrique test site (unpublished data).

5.4 Recharge evaluation

At least 95.4% of the total permeable surface at **Merinos-Colorado-Carrasco** test site presents a moderate recharge, for 43.21 km² of carbonate outcrops the mean recharge rate is 56.7%. Most of it corresponds to surfaces located at high altitude (therefore, with higher rainfall) and intensely karstified areas, at which the carbonaceous materials constitute preferential zones of infiltration (Barberá, 2014). The total recharge obtained through APLIS method for each scenario is presented in Table 5.3.

Table 5.3. Total volumes of recharge at the Merinos-Colorado-Carrasco test site obtained through APLIS.

	Wet (2009/10)	Average (64/65-09/10)	Dry (1998/99)
Total recharge (hm ³ /yr)	29.25	17.96	8.01

Figure 5.7 shows the spatial distribution of specific recharge values, expressed in m³/m². A homogeneous distribution can be observed over the three sierras that compose the study area in the three precipitation scenarios, slightly increasing to the south.

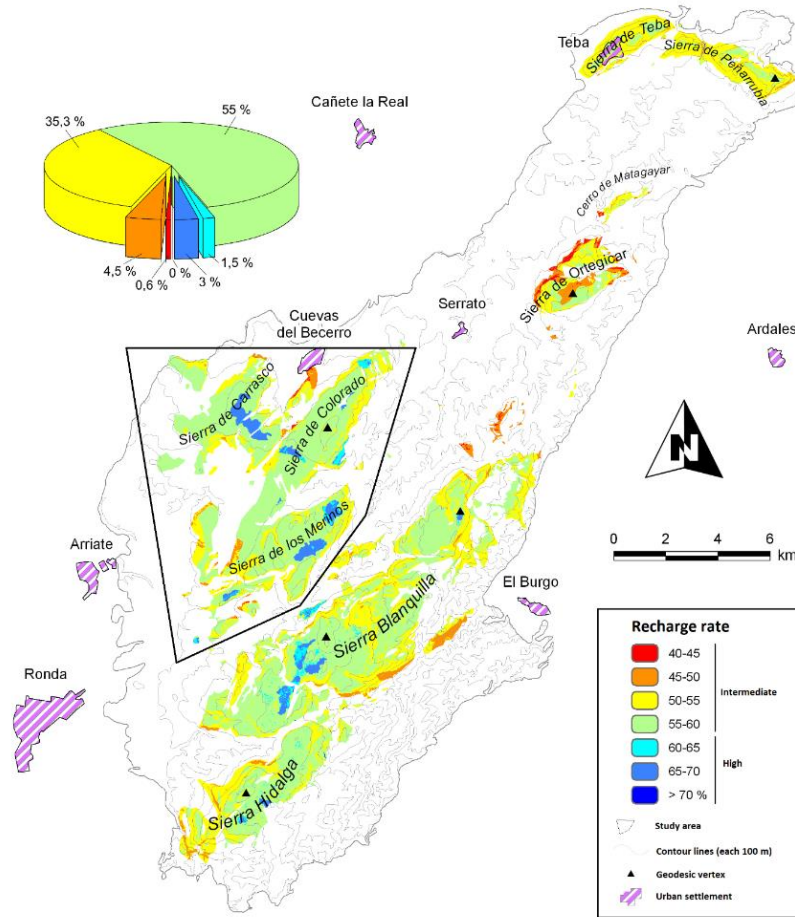


Figure 5.6. Spatial distribution of the recharge rate through the application of the APLIS method at Eastern Ronda Mountains test site.

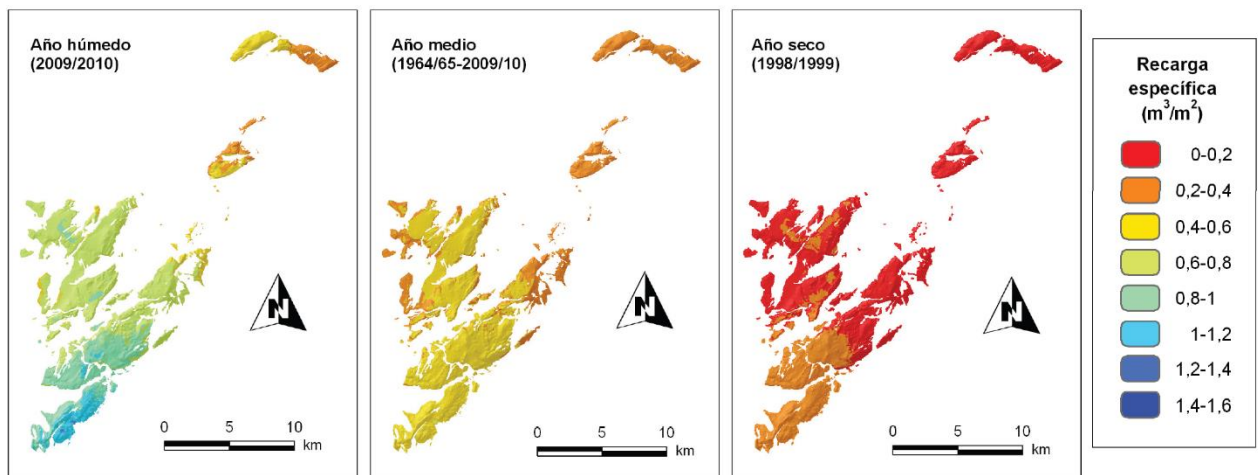


Figure 5.7. Spatial distribution of the specific recharge values at the Eastern Ronda Mountains test site.

In contrast to the main study area, at **Ubrique**, near 97% of the total permeable surface presents a high recharge: for 26.32 km² of carbonate outcrops the mean recharge rate is 72.84%. A common feature with the previous mentioned is that surfaces located at high altitude and areas which present a high grade of karstification constitute preferential zones of infiltration, displaying recharge rate

values > 75%. The only area that shows a recharge rate lower than 60% corresponds to slightly karstified zones in the northern part of the test site.

GIS output layers allow to estimate the total volume of recharge intended for each scenario. As a result, we obtained the values presented in Table 5.4. This test site shows quite similar values in comparison to **Merinos-Colorado-Carrasco**, nevertheless, the recharge area is almost half of the first area.

Table 5.4. Total volumes of recharge at the Ubrique test site obtained through APLIS method.

	Wet (2009/10)	Average (84/85-17/18)	Dry (2004/05)
Total recharge (hm ³ /yr)	45.49	24.47	10.14

Figure 5.10 shows the spatial distribution of specific recharge values, expressed in m³/m². It can be easily observed that it highly depends on the rainfall distribution and altitude, increasing as well to the NE.

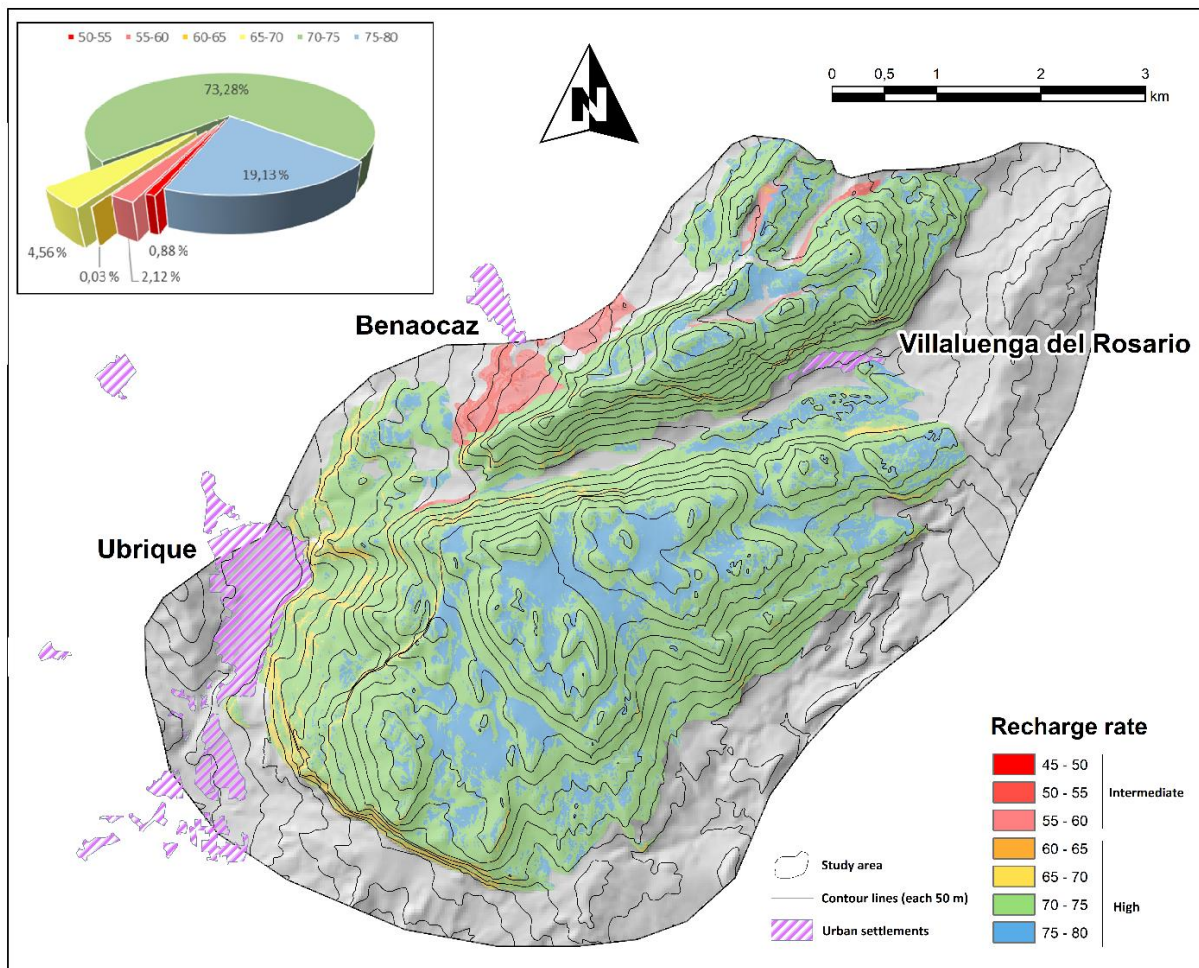


Figure 5.8. Spatial distribution of the recharge rate gained through the application of APLIS in the Ubrique test site.

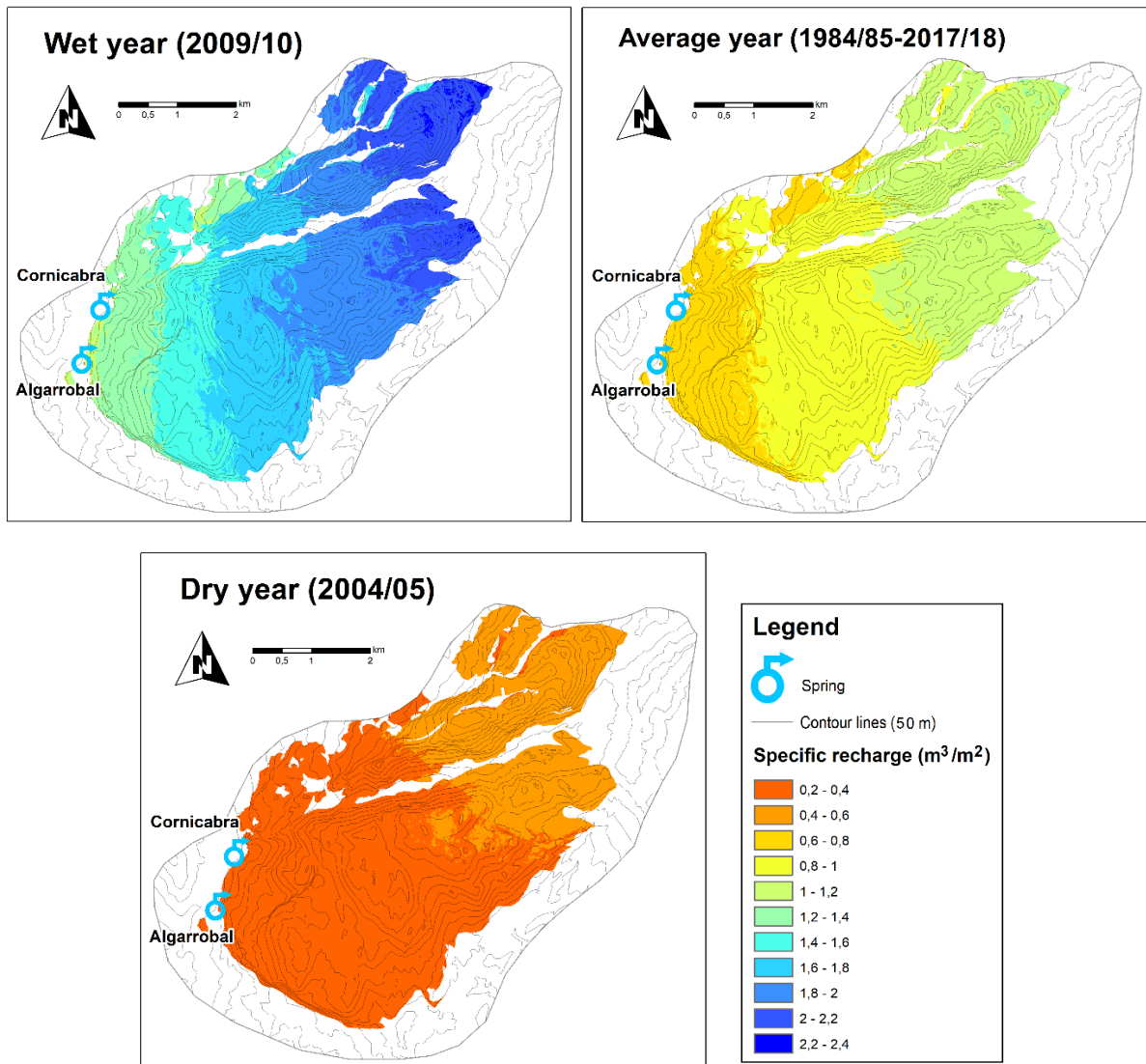


Figure 5.10. Spatial distribution of specific recharge values at the Ubrique test site.

5.5 Discussion and final remarks

As already presented in deliverable 2.1 “Water balance“, the results obtained through the application of APLIS at **Merinos-Colorado-Carrasco** test site nearly coincide with previous research (Tab. 5.5) (Barberá, 2014), which obtained the mean annual recharge through methods different from the one used on this report. In the same PhD Thesis, the recharge rate was also calculated using the methods from Thornthwaite (1948) and Kessler (1967). With the first one, recharge rate was estimated between 64.2% and 72.5%, in contrast, a recharge rate between 54.7% and 56.8% was obtained with the second method, showing quite similar values to those achieved through the APLIS method (17.96 hm³/yr).

Table 5.5. Mean renewable resources (hm³/year) at Merinos-Colorado-Carrasco test site estimated in previous studies (modified from Barberá, 2014).

	Fernández (1980)	IGME (1983)	DPM (1988)	Barberá (2014)
Sierras de Merinos, Colorado y Carrasco	24,3	17,99	17	17,96

Regarding the **Ubrique** test site, the mean annual recharge value obtained through APLIS (24.47 hm³/yr) is consistent with the results previously presented in D2.1 (Tab. 5.6), which was calculated using Thornthwaite's (1948) method and showed a recharge rate value of 75%.

Table 5.6. Estimation of mean annual recharge for the period 2012/15 at the Ubrique test site (modified from Martín-Rodríguez, 2016).

Acuífero	Superficie permeable (Km ²)	Precipitación total (PP), lluvia útil (PU) y evapotranspiración real (ETR). (hm ³)									Media anual		
		2012/13			2013/14			2014/15					
		P	PU	ETR	P	PU	ETR	P	PU	ETR	P	PU	ETR
Ubrique	25,9	56,3	45,1	11,2	39,1	29,2	9,9	29,1	19,8	9,3	41,5	31,4	10,1

In both test sites, Thornthwaite's method tends to overestimate recharge rates compared to other approaches, and thus, the total volume of mean annual recharge is overquantified. APLIS proved to be a robust approach for recharge rate estimation in carbonate aquifers expressed as a percentage of precipitation and allows to reliably establish its spatial distribution, according to the specific features at both test sites.

5.6 References

- Andreo B., Vías J.M., Durán J.J., Jiménez P., López-Geta J.A. & Carrasco F. (2008) Methodology for groundwater recharge assessment in carbonate aquifers: application to pilot sites in southern Spain. *Hydrogeol J* 16: 911–925
- Andreo, B., Vías, J.M., Durán, J.J., Jiménez, P., López-Geta, J.A. and Carrasco, F. (2008). Methodology for groundwater recharge assessment in carbonate aquifers: application to pilot sites in southern Spain. *Hydrogeology Journal* 16 (5), 911-925.
- Barberá, J.A. (2014). Investigaciones hidrogeológicas en los acuíferos carbonáticos de la Serranía Oriental de Ronda (Málaga). PhD Thesis. University of Málaga, Spain. 591 p.
- Barberá, J.A. and Andreo, B. (2012). Functioning of a karst aquifer from S Spain under highly variable climate conditions, deduced from hydrochemical records. *Environ Earth Sci* 65, 2337–2349.
- Kessler, H. (1967). Water balance investigations in the karstic regions of Hungary. Symposium on Hydrology of Fractured Rocks, Dubrovnik (Yugoslavia), AIHS-UNESCO 1, 91-95.
- Marín A.I. (2009) Los Sistemas de Información Geográfica aplicados a la evaluación de recursos hídricos y a la vulnerabilidad a la contaminación de acuíferos carbonatados. Caso de la Alta Cadena (Provincia de Málaga). Tesis de Licenciatura, Universidad de Málaga. 131 pp.
- Martín-Algarra, M. (1987). Evolución geológica alpina del contacto entre las Zonas Internas y Externas de la Cordillera Bética. PhD Thesis, University of Granada, Spain. 1171 p.
- Martín-Rodríguez, J.F., Sánchez-García, D., Mudarra-Martínez, M., Andreo-Navarro, B., López-Rodríguez, M., and Navas-Gutiérrez, M.R. (2016). Evaluación de recursos hídricos y balance hidrogeológico en acuíferos kársticos de montaña. Caso de la Sierra de Grazalema (Cádiz,

España). Book chapter on Las aguas subterráneas y la planificación hidrológica, 163-170. Spanish-Portuguese Congress. IAH Spanish Chapter. Madrid (Spain), November 2016.

Sánchez, D., Barberá, J.A., Mudarra, M. and Andreo, B. (2017). Hydrogeochemical tools applied to the study of carbonate aquifers: examples from some karst systems of southern Spain. *Environmental Earth Sciences*, 74, 199–215.

Thornthwaite, C. W. (1948). An approach toward rational classification of climate. *Geographical Review* 38 (1), 55-94.

6 The Lez Karst Catchment (case study France)

6.1 General description of the test site

The Lez spring catchment is located 15 km north of Montpellier (France). It is located between the Hérault and Virdoule river valleys. The maximum extent of the hydrogeological basin which feeds the Lez spring is estimated to be about 380 km² due to regional drawdown resulting from continuous pumping at the karst spring (Thiéry and Bérard, 1983). The lithology of the Lez karst system corresponds to massive limestone of the Upper Jurassic (Argovian to Kimmeridgian) and of the lower part of the Early Cretaceous (Berriasian), with 650 to 1,000 m thickness. The marls and marly-limestone of the Middle Jurassic (Oxfordian) constitute the lower boundary of the aquifer. The marls and marly-limestone of the Early Cretaceous (respectively Lower and Upper Valanginian) constitute the upper boundary of the aquifer. The major tectonic events that influenced the Lez aquifer were: the Hercynian/Variscan orogeny, the Pyrenees formation, and the opening of the Lion Golf.

As a large part of the hydrogeological catchment is relatively impermeable, due to the presence of marls and marly-limestones of the Valanginian, the Lez spring recharge catchment covers about 130 km² only. The main recharge area over the catchment corresponds to the Jurassic limestone outcrops located by the western and northern limits of the basin. Localized infiltration occurs through fractures and sinkholes along the basin and through the major geologic fault of Corconne-Les Matelles, in the northern part of the basin. A certain number of fractures are also known to exist only just upstream from the Lez spring. The soils on the Lez catchment are essentially leptosols, with some areas of umbrisols in the southern part of the basin. The mean altitude is 191 m. The high altitudes correspond to the Jurassic limestone outcrops in the west and north of the catchment, with the maximum being 655 m. The mean slope is 10%.

The Lez catchment is exposed to a Mediterranean climate, which is characterized by hot, dry summers, mild winters and wet autumns. Analyses by the Météo France show that on average 40% of the annual precipitation occurs between September and November with a high variability across years. The average annual rainfall rate for the 1945-2019 period is 916 mm based on a weighted average of four rainfall stations located on the Lez basin.

6.2 Technical issues about input layers (GIS)

Table 6.1. Input layers for the application of the APLIS method.

Layer	Retrieved from	Resolution	Comments
DEM	BD ALTI®	75m*75m	/
Lithology	BD Charm-50	1/50 000	The BD Charm-50 also contains layers of miscellaneous elements such as faults, karst features, etc.
Soil	BD GSF	1/1 000 000	/
Karst features	BD Charm-50	/	/

6.3 Recharge evaluation

See figures 6.1-6.4.

6.4 Discussion

The results obtained with the APLIS method are consistent with our actual knowledge of the system, especially regarding the main recharge area of the catchment (estimated to 120-150 km² in previous studies):

- We can see on the APLIS recharge map that the main Jurassic limestone outcrops (west and north-west parts of the basin) mostly contribute to the recharge of the aquifer, with a mean recharge rate of 47% for an area of 80 km². The recharge contribution from this area is about 60% of the overall recharge of the catchment.
- Other limestone outcrops among the basin, as well as geological features (major faults and sinkholes), also contribute well to the recharge.

Table 6.2: Estimation of the annual recharge on the Lez catchment according to (i) APLIS method and (ii) a water balance method.

Year	Precipitations (mm)	Annual recharge (Mm ³ /year)	
		APLIS Method	Water balance method
Dry (1952-1953)	438	28.3	10.9
Intermediate (1955-1956)	916	59.5	58.3
Wet (1995-1996)	1763	114.5	161.8

The annual recharge for an intermediate year is estimated at 59.5 Mm³ with the APLIS method and at 58.3 Mm³ with the water balance method. These results are very similar and consistent with the mean annual volume that leaves the system (natural flow at the spring and pumping) estimated at 58.5 Mm³. The annual recharge for a dry year is estimated to be lower with the water balance method (10.9 Mm³ against 28.3 Mm³ with APLIS), which may be related to the evapotranspiration processes that are not considered in the APLIS method. The annual recharge for a wet year is estimated to be higher with the water balance method (161.8 Mm³ against 114.5 Mm³ with APLIS), which is likely due to the run-off volume that is not considered in the water balance method but should be withdrawn to get the effective recharge.

The resolution of the DEM (75 m) may induce some errors regarding the influence of localized recharge points (sinkholes). Indeed, as they are about 2-10 m diameter, they do not necessarily appear on the karst features raster file. The poor resolution of the soil layer (1/1000000) with a large majority of leptosols may induce a slightly overestimation of the recharge rate, as the leptosols are very shallow and have close to zero ability to hold water.

The method seems to provide an accurate estimation of the recharge at the scale of the Lez spring catchment, but we feel that the results could be improved by considering the land cover:

- The urban areas (approximately 20 km²) where the infiltration is insignificant.
- The vegetation, which intercepts a part of the precipitation and releases water from the soil and vadose zone to the atmosphere via the process of transpiration. This volume may be significant, especially in summer where the demand from the vegetation is high and the evapotranspiration is larger than the precipitation.

6.5 Final remarks

The APLIS method seems to provide a consistent estimation of the recharge, by considering many characteristics of the catchment that other methods do not consider (geology, soil, altitude, slope).

Indeed, the estimated annual recharge with APLIS ($\sim 60 \text{ Mm}^3$) is of the same order of magnitude as the mean annual discharge at the Lez spring. Analyses of 18 hydrological cycles of the natural flow of the Lez source (1946-1968) show that the natural state of the system is characterized by an average daily discharge of about $2 \text{ m}^3/\text{s}$, corresponding to an average annual discharge of about $62 \text{ Mm}^3/\text{year}$. Over the same period, the minimum discharge was measured in 1952 with an average daily discharge of about $0,9 \text{ m}^3/\text{s}$, corresponding to an average annual discharge of about $28 \text{ Mm}^3/\text{year}$, which remarkably corresponds to the estimated annual recharge estimated with the APLIS method.

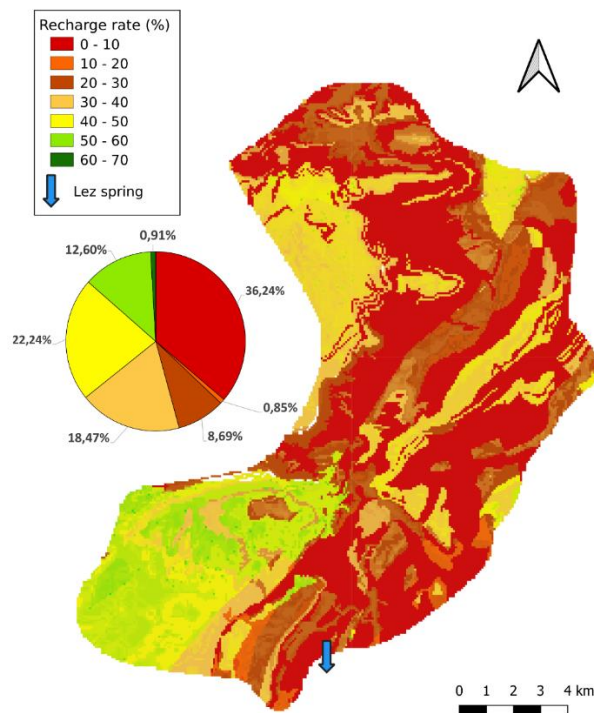


Figure 6.1. Recharge rate (% of total precipitation) on the Lez catchment.

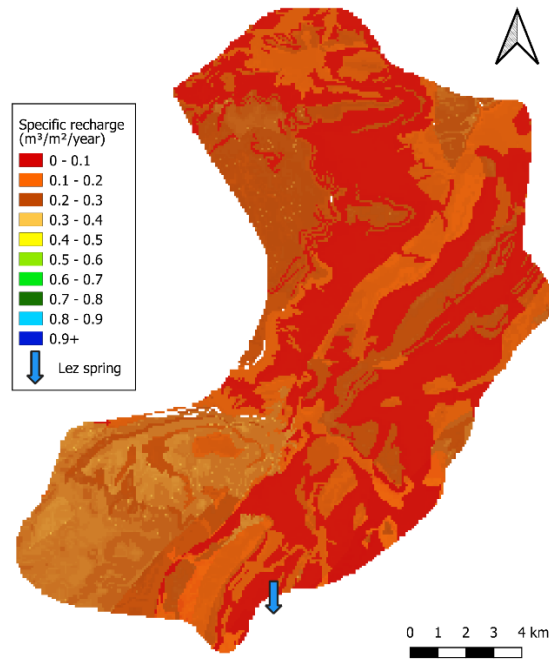


Figure 6.2. Specific recharge ($m^3/m^2/year$) on the Lez catchment for a dry water year (1952-1953).

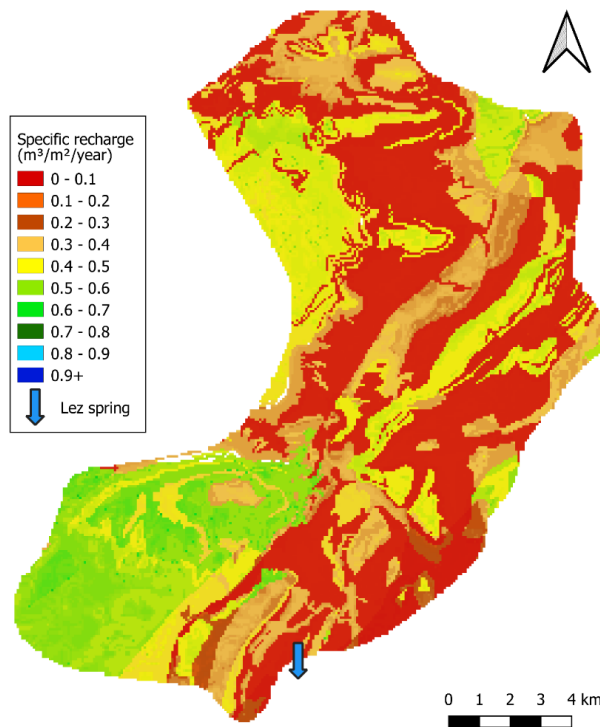


Figure 6.3. Specific recharge ($m^3/m^2/year$) on the Lez catchment for an intermediate water year (1955-1956).

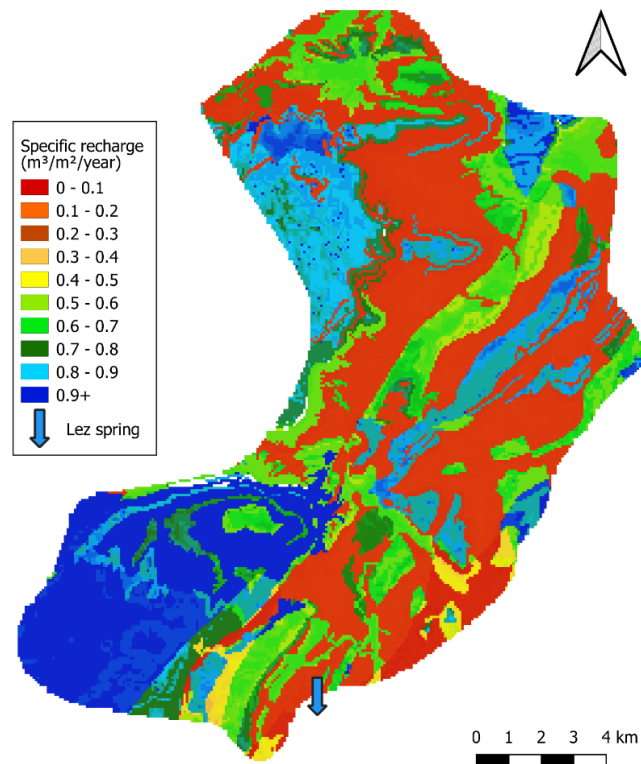


Figure 6.4. Specific recharge (m³/m²/year) on the Lez catchment for a wet water year (1995-1996).

6.6 References

Thiéry, Dominique, et P. Bérard. « Alimentation en eau de la ville de Montpellier - captage de la source du Lez - études des relations entre la source et son réservoir aquifère. » BRGM. SNG 167 LRO, 1983.

7 Hochifen-Gottesacker karst area (test site in Austria)

7.1 Test site

The test site Hochifen-Gottesacker is located in the Northern Alps at the border between Austria (Vorarlberg) and Germany (Bavaria, Fig. 7.1a). The altitude varies between 1035 m asl (Sägebach Spring) and 2230 m asl (summit of Mt. Hochifen). The total size of the catchment area of Aubach- and Sägebach Spring (Fig. 7.1b) is about 35 km² (Chen & Goldscheider, 2014).

The study site belongs to the Helvetic zone, which plunges on three sides underneath the Flysch nappes consisting of marl and sandstone formations (Wyssling, 1986). The most important rock formation is the Cretaceous Schrattenkalk limestone layer, which forms a relatively thin karst aquifer (about 100 m) above a thick marl formation (about 250 m) acting as a regional aquitard. Previous research (Goldscheider, 2005; Goeppert and Goldscheider, 2008) have shown that the orientation of the underground flow paths is structurally controlled, i.e. the underground flow is parallel to the strata. The elevated Gottesacker terrain is a bare karren field, dominated by kluftkarren. In the lower parts, the limestones are covered with shallow rendzina soil, that is partially overgrown with coniferous forest. However, large karst outcrops without overlying soil are frequent (Goldscheider, 2002).

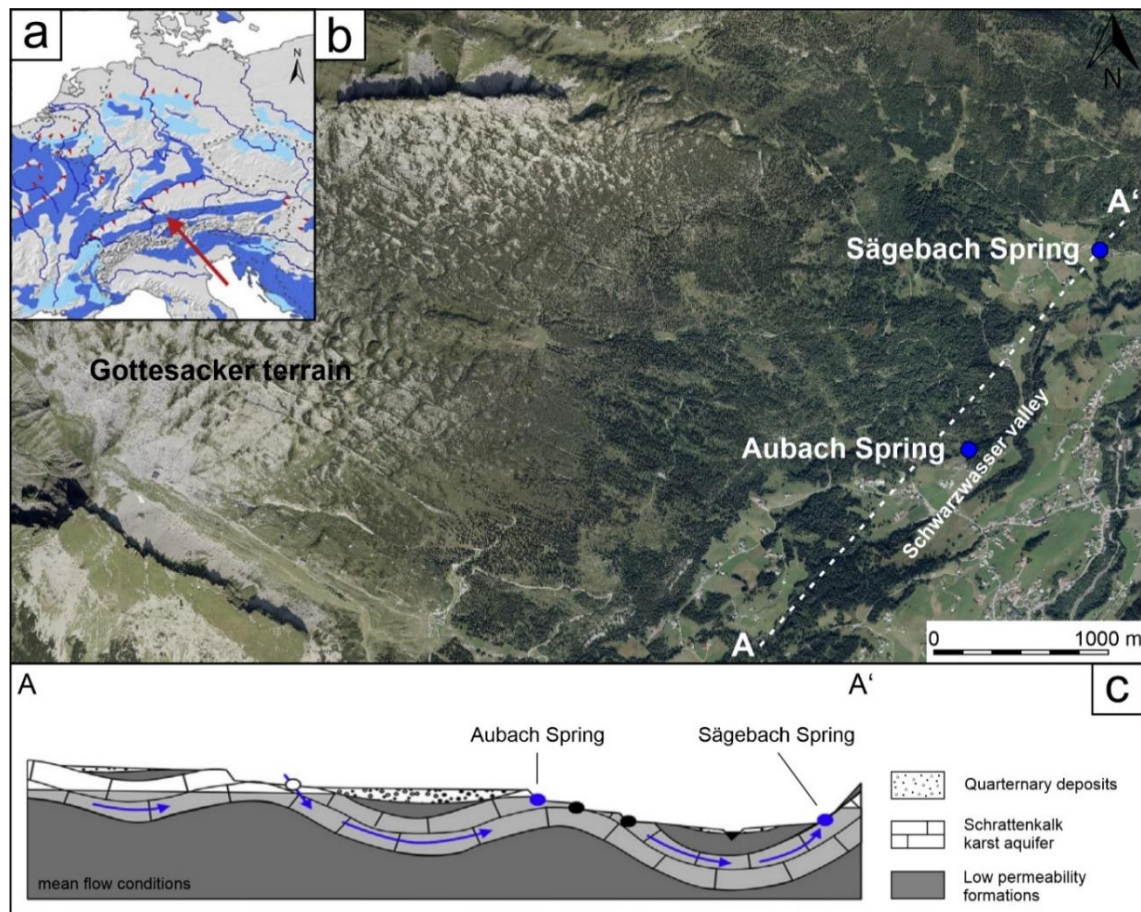


Fig. 7.1. a) Location of the test site shown on a section of the World Karst Aquifer Map (Chen et al., 2017) with carbonate rocks in blue. b) Detail of the test site with the Gottesacker area and Aubach- and Sägebach Spring (basemap: Land Vorarlberg – data.vorarlberg.gv.at) and c) schematic cross-section with flow paths at mean flow conditions (modified after Goepfert et al., 2020).

The mountain range SE of the Schwarzwasser valley is formed by sedimentary rocks of the Flysch zone and is mainly characterized by low permeability and drains by surface runoff. The karst aquifer in the catchment of the springs is recharged directly from precipitation, either diffuse as well as concentrated and also from surface streams that drain the part of the catchment area that consists of low permeable Flysch rocks (Chen & Goldscheider, 2014).

The climate of the study site is cool-temperate and humid. The annual average Temperature at the nearest weather station is 5.7° C while mean monthly temperatures range from 2.2° C to 14.4° C. The mean value of the annual precipitation is 1836 mm, with two maxima in June-August and December-January. Snowfall and snow accumulation usually occur between November and May (Chen et al., 2018).

7.2 Recharge evaluation

Chen et al. (2018) examined the annual variation in groundwater recharge and water storage for the Hochifen-Gottesacker area by using a lumped and distributed modeling approach. While the lumped model represents the water storage in the soil and epikarst, the latter represents the underground karst drainage network and the network of surface streams. Also, the model was updated to consider snow accumulation and the snow melt in spring-time and their influence on groundwater recharge.

Input data consists of hourly discharge data from the main springs and streams and interpolated meteorological data (precipitation, temperature, humidity) from nine weather stations (Chen et al., 2018).

Results for the current conditions (Nov 2013 – Oct 2014; Fig. 7.2) show a precipitation of almost 53 MCM (million cubic meters) and an estimated evapotranspiration of 2.4 MCM leading to a recharge of 44 MCM into the aquifer. 84 % of the 44 MCM is autogenic recharge via diffuse infiltration over the karst area, 16 % is allogenic recharge. With over 80 % of the annual precipitation, the Hochifen-Gottesacker area shows a very high recharge rate. Snow storage is dominant between November and April and subsurface storage between May and October.

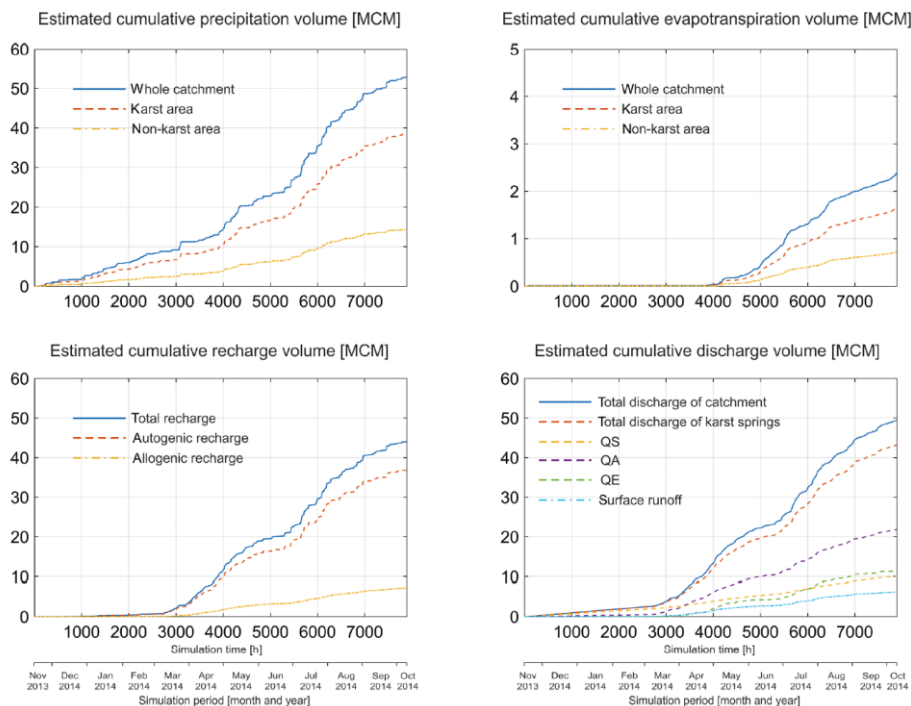


Fig. 7.2. Precipitation, evapotranspiration, recharge and discharge (QS = Sägebach spring, QA = Aubach spring; QE = Estavelle) in the Hochifen-Gottesacker area under current conditions from Chen et al. (2018).

Main focus of this work was to quantify possible effects of climate changes on groundwater recharge and water storage. Results for the future scenarios (overall decreasing discharge in the whole catchment) show that the percentage of snow storage in the cold period decreases significantly, leading to increasing autogenic and allogenic recharge into the karst aquifer. The model predicts increasing recharge in winter and reduced recharge in summer, with both effects offsetting each other. Also, the high recharge rate in the Hochifen-Gottesacker area reduces the impact of rising temperatures and higher evaporation (Chen et al. 2018).

7.3 References

Chen Z, Goldscheider N (2014) Modeling spatially and temporally varied hydraulic behavior of a folded karst system with dominant conduit drainage at catchment scale, Hochifen–Gottesacker, Alps. *Journal of Hydrology*. 514: 41-52.

- Chen Z, Hartmann A, Wagener T, Goldscheider N (2018) Dynamics of water fluxes and storages in an Alpine karst catchment under current and potential future climate conditions. *Hydrol Earth Syst Sci* 22:3807–3823. <https://doi.org/10.5194/hess-22-3807-2018>
- Goeppert N, Goldscheider N (2008) Solute and colloid transport in karst conduits under low- and high-flow conditions. *Groundwater* 46 (1), 61-68.
- Goeppert N, Goldscheider N, Berkowitz B (2020) Experimental and modeling evidence of kilometer-scale anomalous tracer transport in an alpine karst aquifer. *Water Research*, 178.
- Goldscheider N (2002) Hydrogeology and vulnerability of karst systems - examples from the Northern Alps and the Swabian Alb [online]. Ph.D. thesis, 10.5445/IR/1812002
- Goldscheider, N (2005) Fold structure and underground drainage pattern in the alpine karst system Hochiften-Gottesacker. *Eclogae Geol. Helv.* 98 (1), 1–17.
- Wyssling G (1986) Der frühkretazische Schelf in Vorarlberg und im Allgäu - Stratigraphie, Sedimentologie und Paläogeographie. *Jb. Geol. B.-Anst.* 129, 161-265.

8 Conclusions

Aquifer recharge assessment has been successfully performed in selected KARMA test sites and the obtained results are consistent with the recharge evaluation summarized in the previous deliverable D2.1 (Water balance). Nevertheless, slightly different results are observed between APLIS estimations and the different methods used on previous researches presented in D2.1: The APLIS method tends to show somewhat lower recharge values than other methods applied at the different test sites. However, it is necessary to consider that, in some cases, the study period is not contemporary or not long enough to achieve representative results. APLIS has the advantage of using parameters that are not time dependent or changes only occur over long-time scales. Table 8.1 summarizes the results obtained in this report and those obtained through different methods such as Thornthwaite (1957), Kessler (1967), Turc (1954).

Table 8.1. Recharge values obtained at KARMA test sites through APLIS and other methods. a-Turc method, b-Curve-number method, c- Simple linear reservoir model (average from D2.1), d-Kessler method, e-Thornthwaite (field capacity = 50 mm), g-Average of different methods (see D2.1) and h-Lumped and distributed modeling.

Test site	Area (km ²)	APLIS results				Other methods	
		Recharge rate (%)	Wet year (hm ³)	Dry year (hm ³)	Average year (hm ³)	Recharge rate (%)	Average year (hm ³)
Gran Sasso	1034.4	50.6	-	-	500.65	53.97	532.72 ^a
	1080					53.54	546.48 ^b
Qachqouch	55	>60	27.5	22.1	25.6	77.33	44 ^c
East. Ronda Mt.	43.21	56.7	29.25	8.01	17.96	55.79	17.67 ^d
						67.70	25.12 ^e
Ubrique	26	72.84	45.49	10.14	24.47	75.66	31.4 ^e
Lez	150	47 – 60	114.5	28.3	59.5	60 – 65	87.75 ^g
Hochifen-Gottesacker	35					83	44 ^h

The observed limitations of the APLIS method application on KARMA test sites are mainly related to the “I” (infiltration) variable, as it has been evidenced that the development of additional classes is required, as well as the application of a correction factor for urban areas (sealed soils). Another important issue that also needs to be analyzed on depth consists of the combination of APLIS results (recharge rate) and the precipitation layers for each year. The specific recharge map consists of the final output of the method’s application, and thus, the major improvements to come are linked to:

- Snow: the infiltration could suffer a significant delay with respect to the precipitation event date, but only when the snow completely melts from year to year. A different scenario should be considered if a permanent volume of snow exists at the recharge area, so that it does not contribute to the infiltration.

- Dry year case: the dry year case output has shown significant discrepancies at some test sites (like Lez spring) so that the role of evapotranspiration of the vegetation in dry and wet years should be investigated more deeply. A correction factor for vegetation could be included in order to improve APLIS results for dry years and make them more consistent. However, the effect of applying this correction on wet years is still unknown.

These refinements are then focused on improving the accuracy of the precipitation layer, and not the APLIS method itself. The method’s precision can be enhanced by just implementing different correction factors for snow melting, vegetation or soil moisture distribution.

8.1 References

- Goldscheider N (2019) A holistic approach to groundwater protection and ecosystem services in karst terrains. *Carbonates and Evaporites*, 34(4): 1241-1249, doi.org/10.1007/s13146-019-00492-5
- Kessler H (1967) Water balance investigations in the karst regions of Hungary. Act Coll Dubrovnik, AIHS-UNESCO, Paris
- Thornthwaite, C.W. and Mather, J.R., (1957). Instructions and tables for computing potential evapotranspiration and the water balance. *Publ. Climatol.*, 10(3).
- Turc L (1954) The soil balance: relations between rainfall, evaporation and flow (in French). *Geogr Rev* 38:36–44